ENERGY MANAGEMENT OF A MULTI-SOURCE POWER SYSTEM

by

Omar Wasseem Salah

A Thesis Presented to the Faculty of the
American University of Sharjah
College of Engineering
in Partial Fulfillment
of the Requirements
for the Degree of

Master of Science in
Engineering Systems Management

Sharjah, United Arab Emirates

May 2018

Approval Signatures

We, the undersigned, approve the Master's Thesis of Omar Wasseem Salah

Thesis Title: Energy Management of a Multi-Source Power System

Signature	**Date of Signature** (dd/mm/yyyy)
_____	_____
Dr. Abdulrahim Shamayleh Assistant Professor, Department of Industrial Engineering Thesis Advisor	
_____	_____
Dr. Shayok Mukhopadhyay Assistant Professor, Department of Electrical Engineering Thesis Co-Advisor	
_____	_____
Dr. Mostafa Shaaban Assistant Professor, Department of Electrical Engineering Thesis Committee Member	
_____	_____
Dr. Zied Bahroun Associate Professor, Department of Industrial Engineering Thesis Committee Member	
_____	_____
Dr. Mohamed Ben-Daya Director, Engineering Systems Management Graduate Program	
_____	_____
Dr. Ghaleb Husseini Associate Dean for Graduate Affairs and Research College of Engineering	
_____	_____
Dr. Richard T. Schoephoerster Dean, College of Engineering	
_____	_____
Dr. Mohamed El-Tarhuni Vice Provost for Graduate Studies	

Acknowledgment

I would like to express my respect and sincere gratitude to my advisors, Dr. Abdulrahim Shamayleh and Dr. Shayok Mukhopadhyay. Without their endless guidance and genuine encouragement, this work would not have been accomplished. I would also like to express my thanks to the American University of Sharjah for providing me with the opportunity to pursue my graduate studies. I would also like to express my thanks to Ali Al Tamimi for allowing me to conduct an experiment on a ground robot built by him.

Dedication

To my parents

Abstract

Many industries are heavily dependent on fossil fuels to carry out their daily operations. The transportation industry alone is responsible for consuming two thirds of the oil used around the world. As fossil fuel deposits deplete, the need for transportation via sustainable energy solutions such as electric vehicles and battery-powered drones is rising. Battery- operated drones are being targeted by the product delivery industry. However, the use of drones is limited due to constraints on their flight time and distance. This work proposes an energy management system consisting of multiple energy sources integrated into a drone, to optimize the switching between the sources, in an effort to increase the drone's maximum flight time and distance. A mathematical model representing the energy sources in the drone is presented, taking into account the different constraints on the system, i.e. primarily the state of charge of the battery, and super capacitor. In addition to the model, a heuristic approach is developed and compared with the mathematical model. The results generated using both methods are analyzed and compared to a standard mode of the operation of a drone; demonstrating that the dynamic approach provides a superior switching sequence, while the heuristic approach provides the advantage of low computational time. Additionally, the switching sequence provided by the dynamic approach was able to meet the power demand of the drone for all simulations performed and showed that the average power consumption across all sources is minimized. However, switching sequences provided by the heuristic approach and standard mode of operation failed in some simulations. Both the dynamic approach and heuristic approach are also tested on a multi-energy source ground robot built at AUS. The results of the tests are compared to the standard mode of operation of the ground robot; validating that the average power consumption across all sources is minimized by both proposed approaches. Moreover, the concept of scheduling different components in a system to generate the optimal operating sequence, can be used in areas like electric vehicles, and smart homes, by altering the inputs and constraints.

Keywords: ***Batteries; photovoltaic cell; fuel cell; super capacitor; state-of-charge; scheduling; energy management.***

Table of Contents

List of Figures

List of Tables

List of Abbreviations

PV	Photovoltaic cell
SC	Super capacitor
SOC	State-of-charge

Glossary

Photovoltaic cell an electrical device that converts the energy of light from the sun into electricity.

Hydrogen fuel cell an electrochemical cell that converts the chemical energy from a fuel into electricity utilizing an electrochemical reaction between hydrogen and oxygen.

Super Capacitor a high-capacity capacitor with capacitance much higher than typical capacitors.

Chapter 1: Introduction

1.1. Overview

The world currently runs on unsustainable fossil fuels, such as petrol and oil, which emit a remarkable amount of greenhouse gases that harm our environment and result in high levels of pollution. Therefore to limit the levels of pollution, there is a move toward switching to renewable and sustainable energy sources. Additionally our planet has a finite deposit of these fossil fuels and eventually these deposits will be depleted thus resulting in a need to develop sustainable solutions; that can replace the use of fossil fuels which in turn helps ensure a better future for our environment. The Global Footprints organization defines sustainable development as "Development that meets the needs of the present without compromising the ability of future generations to meet their own needs" [1]. Currently, the transportation industry is responsible for consuming the largest amount of fossil fuels where "two thirds of the oil used around the world currently goes to power vehicles, of which half goes to passenger cars and light trucks" [2]. Therefore, a development in this industry resulting in a reduction in the consumption of fossil fuels would have a significant impact on our environment and society. Consequently, companies and governments are eager to find new methods to generate energy that pave the way toward a clean and efficient transportation system [3].

1.1.1. Energy management. The integration of multiple renewable and sustainable sources along with traditional energy sources has become common which creates a need for an efficient energy management of such systems that integrate multiple sources. The main principle in energy management is efficiently matching the demand and supply of power in a system. The main challenge faced is determining in what proportion each of the available sources is used to ensure that enough power is available to meet the demand of the system [4]. This is somewhat tedious because of the different characteristics of the various sources integrated into a multi-source power system. The behaviors of the power sources must be taken into account to achieve efficient management of the sources. Energy management is now being extensively studied in the field of electric vehicles and smart homes, due to the fact that electric vehicles and smart homes usually integrate multiple energy sources such as batteries and photovoltaic cells.

1.1.2. Electric vehicles. In an effort to create a clean and efficient transportation system, research into developing efficient electric vehicles has significantly increased. Electric vehicles now integrate multiple renewable and sustainable energy sources such as batteries, fuel cells, photovoltaic cells, and super capacitors. However, many electric vehicles still include fuel driven motors due to the limitations of renewable sources. Electric vehicles containing merely renewable sources face limitations on the maximum distance they can travel before having to recharge [4]. Therefore, multiple techniques of energy management for electric vehicles have been developed including a dynamic and heuristic approach. The energy management algorithms aim to maximize the usage of the available sources to increase electric vehicles' travel distance.

1.1.3. Drones. Additionally, many companies and countries have turned to the use of drones in their operations, because they are less dependent on fossil fuels for energy. Dubai has conducted its first test of an autonomous drone taxi. The drone taxi has a maximum flight time of thirty minutes, travel distance of fifty kilometers, and a weight limit of one hundred kilograms. The drone taxis are expected to be launched within the next five years in Dubai. Additionally drones are being used by the U.S. military to carry out unmanned attack, by delivery companies to carry out deliveries, as well as by photographers. Also, they are being used in the medical field; for example they are used to deliver automated external defibrillators to out-of-hospital cardiac arrest patients, which can save their life [5]. The technology of drones has improved drastically over the past few years. At the moment, researchers are attempting to incorporate multiple renewable and sustainable energy sources in drones. Drones will integrate multiple sustainable sources such as batteries, fuel cells, photovoltaic panels, and super capacitors. However, the usage of drones has been hindered due to the limitations that these sources face, such as limited energy storage capacity, which affect their flight time and travel distance.

1.2. Problem Statement

As the world turns away from crude energy sources, more sustainable sources like fuel cells are becoming more desirable. Electric vehicles and drones are now incorporating multiple sustainable sources including fuel cells, photovoltaic panels, batteries, and super capacitors which resulted in highly efficient, small-size, light weight, and high performing electric vehicles [6]. For instance, the Dubai

autonomous drone taxi contains nine lithium-ion batteries and smart homes are expected to make use of batteries as well as photovoltaic cells. The integration of multiple sources has been successful with many researchers so far, but there is no consensus on an optimal way of using all the integrated sources simultaneously. Consequently, there are limitations to the range and time that electric vehicles and drones can travel before having to stop and recharge.

The system being studied is a drone that integrates a Hydrogen fuel cell, two batteries, a super capacitor, and a solar panel. The sources will be used to supply the demand of the drone by switching on or off the switches connected to each source.

The proposed study will focus on the optimization of the multiple sources integrated in a drone, to increase the drone's flight time and travel distance. The problem being studied is a resource- constrained scheduling problem of multiple sources incorporated in a drone. The problem will be subject to several constraints, mainly the state of charge of the battery and super capacitor [5]. The objective is to provide an optimal switching sequence between the available energy sources to optimize the performance of the drone.

1.3. Thesis Objectives

The system being studied in this thesis is a drone that contains four different power sources. These sources are a hydrogen fuel cell, two batteries, a solar panel, and a super capacitor. The usage of each of the sources is controlled by turning connected switches on or off as needed to supply the demand of the system. The use of the sources should be optimized, to ensure that the drone could travel the longest distance possible before having to stop to land safely and recharge. As a result, there is a need to optimize the scheduling of the switching sequence of the sources in order to minimize the power dissipation in the drone and increase its travel time. Therefore, the different components in the drone will be modeled to generate the optimal sequence of the switching between the sources. The generated optimal sequence will be tested mainly on MATLAB and LINGO. We are developing an optimized energy source scheduling mathematical model in addition to a heuristic procedure, which have the potential to be implemented in future on a drone. Certain simulations will also be performed for a drone, by assuming a particular flight energy profile. The switching sequences generated will also be tested on a ground robot built in AUS.

1.4. Research Significance

The success of this research would provide a pathway for future projects as well. The concept of scheduling different components in a system to generate the optimal operating sequence could be used in many areas. By altering the inputs and constraints, this algorithm could be used to optimize the operations of electric vehicles, smart homes, and many more applications.

1.5. Methodology

The following steps were taken to accomplish the outcomes proposed in this paper:

Step 1: Review the literature related to different techniques used in optimizing the use of multiple energy sources in electric vehicles and drones.

Step 2: Formulate a mathematical model representing the sources integrated in a drone by defining the assumptions, parameters, decision variables, objective function, and constraints related to the problem to increase the drone's flight time. The mathematical model will be used to schedule the sources to provide the required power while satisfying the system's constraints.

Step 3: Code the formulated model using LINGO optimization software to find the optimal sequence of switching between the integrated energy sources to maximize the usage of the sources.

Step 4: Develop a heuristic approach which will be coded and solved MATLAB to generate a sequence of switching between the integrated energy sources to maximize the usage of the sources.

Step 5: Compare the performance of the dynamic approach, heuristic approach, and standard method of operation.

Step 6: Perform a sensitivity analysis to check the effect of varying the drone's model inputs on the optimal solution.

Step 7: Test the scheduling algorithm on the ground robot built in the American University of Sharjah.

1.6. Thesis Organization

Previous work related to drones, battery modeling, fuel cell modeling, super capacitor modeling, usage of power electronics, control strategies, and scheduling methods are discussed in Chapter 2. The mathematical model developed representing the sources integrated in a drone is discussed in Chapter 3 along with the system constraints. The heuristic algorithm developed to solve the mathematical model is

explained in Chapter 4. The simulation results and sensitivity analysis is discussed thoroughly in Chapter 5. Finally, Chapter 6 provides a summary and contribution of the work.

Chapter 2: Literature Review

In this section we will review previous work related to drones, battery modeling, fuel cell modeling, super capacitor modeling, usage of power electronics and control strategies. It will also demonstrate different scheduling methods used to optimize the integration of multiple sources in electric vehicles; including predictive programming, convex programming, real-time programming, online strategies, and heuristic algorithms.

2.1. Drones

Nowadays, drones are used for a number of applications. Drones have been effectively used in disaster management, and parcel delivery [5]. In Parcel delivery, the delivery time can be reduced because drones are not yet significantly affected by the infrastructure of the city including; traffic lights and traffic volume. Nevertheless, the main constraint that drones encounter is their limited flight time and the total distance they can travel. Most commercial drones are equipped with only single lithium-ion battery that allows a maximum flight time of about thirty minutes, mostly less [7]. Therefore, integrating multiple sustainable sources in drones will aide in increasing their flight time.

Integrating sustainable sources and optimizing their usage, will maximize the drone's performance. Currently, energy management techniques specific to optimizing the use of multiple sources in drones are limited as drones are relatively new compared to electric vehicles. However, Banerjee & Roychoudhury suggest an approach inspired by the "Price Theory" in Economics [7]. The Price Theory states the price of goods in the market can be determined by the supply and demands of those goods. The researchers suggest that the battery's power to be distributed among the different tasks to be completed by the drone. Each task receives a limited amount of power, based on the priority of the task. By doing so, it may be possible that the drone will have excess power to react to unforeseen circumstances such as crashes or sustaining damage to its hardware which occur quite often in drone operations [7]. Additionally, many researchers are studying how drones can be incorporated in delivery systems to reduce the delivery times of products to customers. Ferrandez et al studied a truck-drone delivery using k-means clustering to find optimal launch sites for their drones and a traveling salesman problem to find optimal truck routes [8]. They concluded that the

total delivery time is reduced when introducing drones to the delivery system as opposed to standard truck delivery system. The researchers also suggest battery swaps for the drones on trucks and solar charging stations to increase the flight time of drones, which still represents a limitation.

2.2. Scheduling Approaches

This section will show the different methods researchers have used to optimize the usage of multiple integrated sources in electric vehicles such as predictive and real-time programming. Both electric vehicles and drones face limitations on the maximum distance they can travel and integrate multiple sustainable energy sources. Therefore methods used on electric vehicles can be applied to drones to increase their maximum flight time and flight distance.

2.2.1. Predictive programming. Many researchers are exploring various way on managing the energy generated from multiple energy sources. Torreglosa et al. used predictive control to manage the energy generated from a fuel cell, battery, and super capacitor to operate a tramway in Spain [9]. They modeled their system based on commercially available components and ran simulations using Matlab. The predictive control used previously collected data on the tramway's operation to generate a sequence of operations of the three sources. Based on the demand on the tramway, the controller generates reference currents for both the fuel cell and the battery. The predictive controller repeatedly takes measurements of the tramway's current state. Using previous measurements along with current measurements, the controller calculates the optimal references for the sources to efficiently supply the demand of the tramway. This is done while considering certain constraints including the state of charge of both the battery and super capacitor as well as the allowed current range of the fuel cell. Additionally, Xie et al. compared a stochastic predictive control model on an electric bus to the traditional dynamic programming with no prediction [10]. The electric bus has two sources of energy; the battery and an engine that uses petrol. The stochastic predictive control model uses Markov Chain Monte Carlo methods to predict the future velocities of the bus. The forecasted velocities are then input into a dynamic programming algorithm to provide the optimal control sequence to minimize the energy consumption of the bus, while taking into consideration the state of charge of the

battery. The results showed that dynamic programming provided a lower consumption of fuel as compared to the stochastic predictive control model.

2.2.2. Convex programming. Similarly, Hu et al. used convex programming on a hybrid bus, integrating a fuel cell and battery, to optimize the power management and sizing of the sources [11]. The researchers modeled the fuel cell to take into account the main fuel stack and the four auxiliary systems, air supply system, water management system, cooling system, as well as the hydrogen storage and supply system. They included a scaling factor while modeling the power output of the fuel cell system and modeled the mass of the fuel cell to study the effect of the size of the system on the operation of the hybrid vehicle. The power output of the battery in the hybrid vehicle is also modeled, while also considering the effect of the rating and mass of the battery on the performance of the vehicle. The researchers also considered the limitations of the currents of both the fuel cell system and the battery as well as the desired range of the state of charge of the battery. The researchers also studied the influence of the driving patterns of the bus driver and the prices of the components used in their model on their optimized result [11]. Hadj-Said et al. also used convex programming for the energy management of an electric powertrain [12]. The researchers used a convex model of the powertrain to minimize the fuel consumption of the vehicle. Hadj-Said et al. compared their results to the traditional dynamic programming; convex programming provides an optimal solution close to that of the dynamic programming. However, the use of convex programming provided one advantage of requiring a lower computation time compared to the dynamic programming.

2.2.3. Real-Time programming. Another method for scheduling sources in electric vehicles is real-time programming. Trovão et al. developed a real-time energy management architecture for electric vehicles using two different sources [13]. This system provides an optimal real-time management of the two sources, without previously having access to the demand profile of the vehicle. The researchers divided the real-time management architecture into two categories: the high level of energy management and the middle level of power management. At the high level, the energy management system restricts its search for the optimal solution considering the capabilities of the available sources. The objective of this level is to preserve the battery's state of charge by trying to rely heavily on the super capacitors to meet the

demand of vehicle. The middle level of the energy management system is used to ensure that the power supply is uninterrupted and minimize the difference in the power demanded and power supplied. Trova et al. also studied another real- time energy management approach using a fuzzy logic controller approach on a three wheeled vehicle [14]. In this approach, a super capacitor is combined with a battery in an electric vehicle. The battery is responsible for supplying the average power demand of the vehicle, while the super capacitor provides the rest of the required energy. Using MATLAB/SIMULINK, the researchers found that there was a 3% reduction in energy consumption by the vehicle and battery current RMS value was reduced by 12%. This reduction in the battery's current RMS value helps increases the lifetime of the battery and size of the battery needed. This approach can be adjusted by simply adjusting the expressions used to suit any vehicle, including drones.

2.2.4. Online strategy. Zhou et al. [15] propose an Online Energy Management strategy that combines both an online and offline approach test on hybrid vehicle consisting of a fuel cell and battery. The online energy management is based on time series prediction model nonlinear autoregressive neural network, NARANN. The nonlinear model accepts dynamic inputs of time series sets using a moving window method. The data collected is used to predict the driving cycle of the next window. After the data is collected, offline optimized-based strategies are used to optimize the use of the sources in the next window. By using this method, the researchers were able to optimize the use of the sources. Additionally, Chen et al. implemented an online energy management on a hybrid electric vehicle to reduce the energy consumption of the vehicle [16]. The online energy management strategy is divided into two layers. The first layer is used to determine whether the battery alone or the battery and engine will supply the demand of the vehicle. The second layer of the strategy is used for the power allocation between the battery and engine when both sources are being used based on a sequence generated by dynamic programming. Under specific driving conditions, the researchers were able to reduce the energy consumption up to 5.77%.

2.2.5. Heuristic Algorithm. Another approach researchers are studying is the heuristic approach to the assignment of batteries in order to supply the demand in drone systems. Park et. Al use a greedy heuristic to assign batteries and chargers of drones to services with a temporal order, find the optimal charging schedule, and task dispatching [17]. The researchers divide the batteries and services into categories depending on the required energy to complete tasks and the battery capacity of the drones. Park et. Al also used integer linear programming to schedule the charging of batteries and dispatching of drones to complete their tasks. While scheduling the charging and dispatching, the researches took into account the battery maximum and minimum states of charge to protect the battery's life and not degrade the battery. Also, Umetani et al. used a linear programming based heuristic algorithm for charging and discharging scheduling of electric vehicles [18]. The algorithm consists of two steps: solving the linear programming problem, and rounding the optimal solution to obtain feasible integer solutions. The heuristic algorithm was able to reduce the peak load of the vehicle while also handling the uncertain demands of the electric vehicle with minimal computation time.

2.3. Battery Modeling

One crucial factor to the success of portable electronics, is the battery's power dissipation and runtime. Chen and Rincon-Mora present in their research an accurate and efficient battery model that could help researchers predict and optimize the battery's runtime as well as the overall system performance [19]. The model accounts for various dynamic characteristics of a battery including open-circuit voltage, current, temperature, and many more. While testing their model, the researchers observed less than 0.4% runtime error and a mere 30 mV error in the voltage. While designing hybrid systems, consisting of fuel cells along with batteries and super capacitors, the battery is selected based on its energy requirements to reduce its size and weight. This does not take into account the deep discharges of the battery which have a significant effect on the battery's lifetime. Therefore Schaltz, Khaligh, and Rasmussen argue that alongside the energy and power requirements of the battery, the lifetime of the battery must be considered too [20].

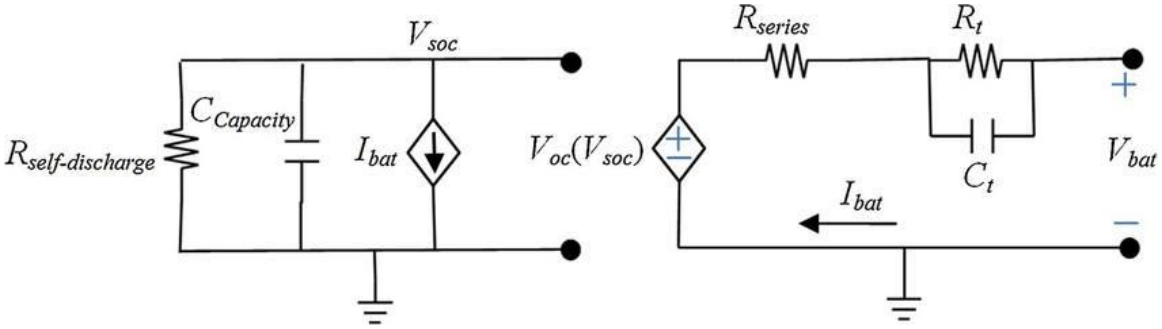

Figure 1: Electrical circuit model of battery [19].

2.4. Fuel Cell Modeling

Another aspect of the system that must be modeled and managed is the fuel cell to minimize the hydrogen consumption to insure appropriate runtime. Bernard et al. investigate the effects of the sizing and modeling of the fuel cells in a powertrain powered by fuel cell and energy storage systems [21]. They examine different combinations of fuel cell models alongside energy storing systems to determine which combination results in the least hydrogen consumption to increase the runtime of the powertrain. Pukrushpan states that the efficiency of fuel cells depends on understanding, predicting, and controlling the distinctive performance of fuel cell systems [22]. In this thesis, Pukrushpan provides a number of modeling and controlling techniques that can be used to insure quick and stable dynamic system behavior. As well as considering various limitations of the controlling techniques discussed and ways to measure the performance of the fuel cell system.

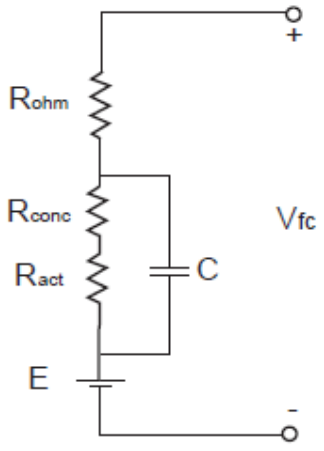

Figure 2: Fuel cell equivalent circuit [21].

2.5. Super capacitor Modeling

Super capacitors are being used more frequently in hybrid vehicles because of their ability to provide a quick burst of current needed during acceleration [6]. Spyker & Nelms explain how to model a super capacitors so that it can be used to describe the performance of the capacitor [23]. They consider the internal heating of the super capacitor when charged, equivalent parallel resistance, and equivalent series resistance and how they affect the performance and discharge of the capacitor. Additionally, Amjadi & Williamson add that a super capacitor can be used to supply the excess instantaneous power needed by a hybrid system [24]. By doing so, the battery's lifetime can be protected and the dynamic stress on the battery is reduced by the help of the super capacitor.

2.6. Power Electronics and Control Strategies used in Hybrid Electric Vehicles

Hybrid electric vehicles generally contain four sources; the battery, fuel cell, photovoltaic panels, and a super capacitor. These sources provide direct current (DC) power, but most motors used in vehicles require alternating current (AC) power. Therefore, an inverter is needed to change the DC power coming from these sources to AC power. Additionally, the voltage generated from these sources is not constant. The voltage might be higher than the required value when the source is completely charged or lower than the required value when the source's state-of-charge drops. The voltage drops as the source is depleted and requires to be charged again. Consequently, a DC/DC Buck-Boost converter is connected to these sources to insure that the voltage supplied to the inverter is of the required value [25]. All three sources could be connected to one DC/DC converter then to an inverter to supply the motor as shown in the figure below:

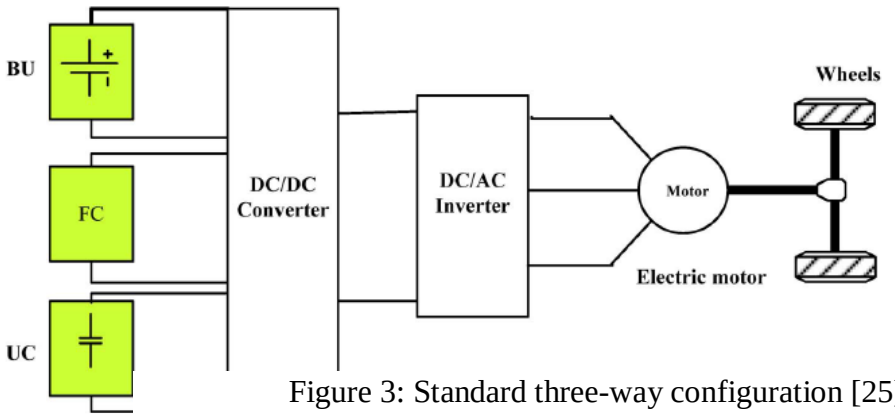

Figure 3: Standard three-way configuration [25].

Typically in HEVs, a reference signal is generated to indicate the current required by the electric vehicle to supply the demand of the vehicle. One reference signal is used to control the operations of the fuel cell, also taking into account the state-of-charge of the battery and super capacitor, as well as the output of the solar panel [25]. Using the reference signal, the algorithm can decide which of the four sources is needed to supply the vehicle or even if all four sources must supply simultaneously.

Chapter 3: System's Model

The objective of this research is to develop and solve a mathematical model that will provide a switching sequence between the energy sources of a drone. Consequently, the solution of this mathematical model will optimize the drone flight time and distance traveled.

3.1. Model Assumptions

The proposed model assumes the following:

1. The initial state of charge of the battery is 100%.
2. The initial state of charge of the super capacitor is 100%.
3. The hydrogen tank of the fuel cell is full.
4. The batteries can only be charged by the photovoltaic cell.
5. The super capacitor can be charged either the batteries or the photovoltaic cell.

3.2. Problem Parameters and Subscripts

The subscripts used in the proposed model are:

$\mathbf{B_1}$	Battery #1
$\mathbf{B_2}$	Battery #2
C	Super capacitor
PV	Photovoltaic cell
Fc	Fuel cell

The parameters of the proposed model are:

N	Number of time steps
k	Time step, k=1,2…,N
Δ**t**	Step size
i	Battery index $\forall$ i{1,2}
$\boldsymbol{\tau}$	Time constant of the super capacitor.
w	weight assigned to each of the sources in the objective function.

3.3. Problem Decision Variables

The following are the decision variables of the mathematical model:

$\mathbf{S_{Bi}(k\Delta t)}$ A binary variable that equals 1, if battery i is supplying the demand of the system at time step $k\Delta t$, 0 otherwise.

$\mathbf{ch_{Bi}(k\Delta t)}$ A binary variable that equals 1, if battery i is being charged from the system time step $k\Delta t$, 0 otherwise.

$\mathbf{S_C(k\Delta t)}$ A binary variable that equals 1, if the super capacitor is supplying the demand of the system at time step $k\Delta t$, 0 otherwise

$\mathbf{ch_C(k\Delta t)}$ A binary variable that equals 1, if the super capacitor is being charged from the system at time step $k\Delta t$, 0 otherwise.

$\mathbf{S_{pv}(k\Delta t)}$ A binary variable that equals 1, if the photovoltaic cell is supplying the demand of the system at time step $k\Delta t$, 0 otherwise

$\mathbf{S_{fc}(k\Delta t)}$ A binary variable that equals 1, if the fuel cell is supplying the demand of the system at time step $k\Delta t$, 0 otherwise

The following are variables that are calculated based on the decision variables:

$\mathbf{SOC_{Bi}(k\Delta t)}$ State of charge of the battery i at time step $k\Delta t$.

$\mathbf{SOC_C(k\Delta t)}$ State of charge of the super capacitor at time step $k\Delta t$.

$\mathbf{V_{Bi}(k\Delta t)}$ Voltage of the battery i at time step $k\Delta t$.

$\mathbf{i_{Bi}(k\Delta t)}$ Current of the battery i at time step $k\Delta t$.

$\mathbf{P_{Bi}(k\Delta t)}$ Power supplied by the battery i at time step $k\Delta t$.

$\mathbf{V_C(k\Delta t)}$ Voltage of the super capacitor at time step $k\Delta t$..

$\mathbf{I_C(k\Delta t)}$ Current of the super capacitor at time step $k\Delta t$.

$\mathbf{P_C(k\Delta t)}$ Power supplied by the super capacitor at time step $k\Delta t$.

$\mathbf{P_{PV}(k\Delta t)}$ Power supplied by the photovoltaic cell at time step $k\Delta t$.

$\mathbf{V_{FC}(k\Delta t)}$ Voltage of the fuel cell at time step $k\Delta t$.

$\mathbf{I_{FC}(k\Delta t)}$ Current of the fuel cell at time step $k\Delta t$.

$\mathbf{P_{FC}(k\Delta t)}$ Power supplied by the fuel cell at time step $k\Delta t$.

$\mathbf{P_{demand}(k\Delta t)}$ Power demanded by the system at time step $k\Delta t$.

3.4. Model Formulation

- **Objective Function**

$$\boldsymbol{Min} \sum_{k=1}^{N} \boldsymbol{w_{B1}P_{B1}}(\mathbf{k\Delta t})\big(\mathbf{1}-\boldsymbol{ch_{B1}}(\mathbf{k\Delta t})\big)+\ \boldsymbol{w_{B2}P_{B2}}(\mathbf{k\Delta t})\big(\mathbf{1}-\boldsymbol{ch_{B2}}(\mathbf{k\Delta t})\big) + \boldsymbol{w_{C}P_{C}}(\mathbf{k\Delta t})\big(\mathbf{1}-\boldsymbol{ch_{C}}(\mathbf{k\Delta t})\big)+\boldsymbol{w_{PV}P_{PV}}(\mathbf{k\Delta t}) + \boldsymbol{w_{FC}P_{FC}}(\mathbf{k\Delta t}) \quad \$ \tag{1}$$

The objective function (1) will minimize the running cost of the system. The system being studied contains five sources; two batteries, a fuel cell, a photovoltaic cell, and a super capacitor. If the batteries or the super capacitor are being charged, the power used to charge these sources will not be considered in the objective function. For instance if the first battery is being charged from the photovoltaic cell, the power consumed by the battery and supplied by the photovoltaic cell will not be considered in the objective function. Therefore, the power provided by the batteries and super capacitor is multiplied by a factor, (1- $ch_i(t)$), made equal to zero when one of these sources is being charged as shown in the objective function above. These sources do not behave in the same manner, each has their own unique characteristics and running costs. A weighting system will be used to account for these differences developed using an analytic hierarchy process, AHP, presented in section 3.5. The power supplied by each of the sources will be multiplied by the assigned weight to it; w_{B1}, w_{B2}, w_C, w_{PV}, w_{FC} as shown in the objective function. As an example we are considering the weights to be \$/W, but they can be any monetary unit.

- **Battery Model**

$$SOC_{Bi}(\mathrm{k\Delta t}) = \frac{-1}{C_C} I_{Bi}(\mathrm{k\Delta t})\big(S_{Bi}(\mathrm{k\Delta t}) - ch_{Bi}(\mathrm{k\Delta t})\big) + SOC_{Bi}((k-1)\Delta t)\ \forall k \tag{2}$$

The state of charge (SOC) of the battery will be calculated continuously as the system is running using equation (2).

$$I_{Bi}(\mathrm{k\Delta t}) = I_{Brated}\ \forall k\ \ \mathrm{A} \tag{3}$$

The current of the battery will be calculated using equation (3). The battery will be operated at rated conditions, providing the maximum continuous current.

$$P_{Bi}(\mathrm{k\Delta t}) = V_{Bi}(\mathrm{k\Delta t}) I_{Bi}(\mathrm{k\Delta t}(S_{Bi}(\mathrm{k\Delta t}) + ch_{Bi}(\mathrm{k\Delta t}))\forall k\ \mathrm{W} \tag{4}$$

The assumption of a constant voltage is valid because a voltage regulator will be present. Therefore, the power provided by the battery will be calculated using equation (4).

- **Battery Constraints**

$$S_{Bi}(\mathrm{k}\Delta\mathrm{t}) + ch_{Bi}(\mathrm{k}\Delta\mathrm{t}) \leq 1 \quad \forall k \tag{5}$$

Constraint (5) ensures that both batteries are either charging, supplying, or the system is left idle at each time step k.

$$ch_{B1}(\mathrm{k}\Delta\mathrm{t}) + ch_{B2}(\mathrm{k}\Delta\mathrm{t}) \leq 1 \forall k \tag{6}$$

Constraint (6) ensures that only one of the batteries is charged at time step k.

$$30\% \leq SOC_{Bi}(k\Delta\mathrm{t}) \leq 100\% \; \forall k \tag{7}$$

Constraint (7) ensures that the state of charge of the batteries stays between 30% and 100% to protect the lifetime of the battery.

- **Super Capacitor Model**

$$\tau = \mathrm{RC} \tag{8}$$

The time constant of the super capacitor is calculated using equation (8).

$$V_C(\mathrm{k}\Delta\mathrm{t}) = V_s(1 - e^{\frac{-\mathrm{k}\Delta\mathrm{t}}{\tau}})ch_C(\mathrm{k}\Delta\mathrm{t}) \quad \forall k \text{ V} \tag{9}$$

When the super capacitor is charging, the voltage will be calculated using equation (9).

$$V_C(\mathrm{k}\Delta\mathrm{t}) = V_C((\mathrm{k}-1)\Delta\mathrm{t})e^{\frac{-\mathrm{k}\Delta\mathrm{t}}{\tau}}S_C(\mathrm{k}\Delta\mathrm{t}) \; \forall k \text{ V} \tag{10}$$

When the super capacitor is supplying the system, the voltage will be calculated using equation (10).

$$V_C(\mathrm{k}\Delta\mathrm{t}) = V_C((\mathrm{k}-1)\Delta\mathrm{t})(1 - (S_C(\mathrm{k}\Delta\mathrm{t}) + ch_C(\mathrm{k}\Delta\mathrm{t}))\forall k \text{ V} \tag{11}$$

If the capacitor is left idle, the voltage will remain the same as shown in equation (11).

$$I_C(\mathrm{k}\Delta\mathrm{t}) = \frac{C \cdot Vs}{\tau} \cdot e^{\frac{-t}{\tau}} \cdot chc(\mathrm{k}\Delta\mathrm{t}) + \frac{C \cdot Vc(t-1)}{\tau} \cdot e^{\frac{-t}{\tau}} \cdot Sc(\mathrm{k}\Delta\mathrm{t})\forall k \text{ V} \tag{12}$$

The current of the super capacitor will be calculated using equation (12).

$$P_C(\mathrm{k}\Delta\mathrm{t}) = I_C(\mathrm{k}\Delta\mathrm{t})V_C(\mathrm{k}\Delta\mathrm{t})(\, S_C(\mathrm{k}\Delta\mathrm{t}) + ch_C(\mathrm{k}\Delta\mathrm{t}))\forall k \;\; \mathrm{W} \tag{13}$$

The power provided by the super capacitor will be calculated using equation (13).

$$SOC_C(\mathrm{k}\Delta\mathrm{t}) = \frac{V_C(\mathrm{k}\Delta\mathrm{t})}{V_{Crated}} \ \forall k \quad (14)$$

The state of charge (SOC) of the super capacitor will be calculated continuously as the system is running using equation (14).

The sizing of the super capacitor is based on the rush of current needed during spikes in the demand of the drone. A spike in the drone's demand can occur due to a sudden increase in the drone's traveling altitude. Therefore, the size of the super capacitor needed can be found as follows:

The energy E needed to raise an object of mass m a height h is:

$$E = mgh \ \text{J} \quad (15)$$

Where g is the gravitational acceleration.

By definition, 1 joule is equal to 1 volt multiplied by 1 coulomb. Therefore:

$$E = QV \ \text{J} \quad (16)$$

Where Q is the charge of the super capacitor in coulombs and V is the voltage in volts.

Additionally, the charge of the capacitor is dependent on the capacitance and voltage:

$$Q = CV \ \text{C} \quad (17)$$

Where C is the capacitance in Farads.

Therefore, by using equations (15) & (16) & (17) the following equation (18) can be used to determine the size of the super capacitor need. A safety factor could also be considered to insure that the super capacitor can handle any spikes of demand resulting from turbulences encountered during the flight,

$$C = \frac{mgh}{V^2} \ \text{F} \quad (18)$$

- **Super Capacitor Constraints**

$$S_C(\mathrm{k}\Delta\mathrm{t}) + ch_C(\mathrm{k}\Delta\mathrm{t}) \leq 1 \ \forall k \quad (19)$$

Constraints (19) ensures that the super capacitor either charging, supplying, or the system is left at each time step k.

- **Photovoltaic Cell Model**

$$P_{PV}(k\Delta t) = S_{PV}(\mathrm{k\Delta t})\mathrm{PV}(\mathrm{k\Delta t})(1 - [ch_{B1}(\mathrm{k\Delta t}) + ch_{B2}(\mathrm{k\Delta t}) + ch_{C}(\mathrm{k\Delta t})])\forall k\mathrm{W} \quad (20)$$

The profile of the photovoltaic cell, PV(kΔt), will be uploaded into the system via a controller and its output will be determined using equation (20). The controller in the system contains two level; an upper and lower level. The lower level is responsible for using the GPS coordinates of the drone's destination to adjust the motors of the drone as needed. On the other side, the upper level of the controller deals with the load profile of the drone and the photovoltaic cell's profile. Additionally, the switching sequence generated by the proposed model will be uploaded to the system via the upper level of the controller. Therefore, the photovoltaic cell can either be supplying the demand of the system or charging one of the batteries.

- **Fuel Cell Model**

Figure 4 shows an individual fuel cell and a fuel cell stack. Individual fuel cell are typically stacked together to achieve a greater voltage and= power output.

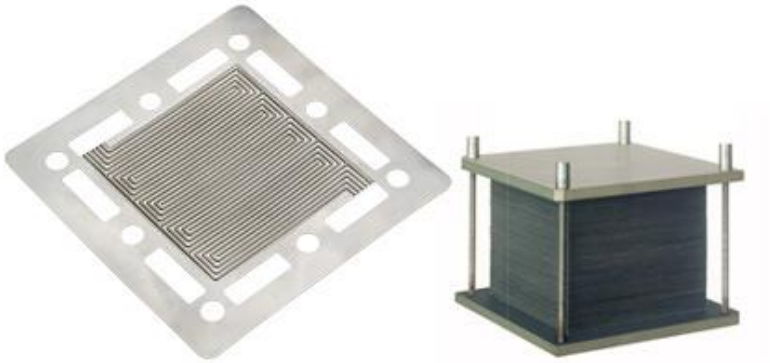

Figure 4: Individual fuel cell and fuel cell stack [26]

$$I = \frac{I_{st}}{A_{fc}}\ \mathrm{A} \quad (21)$$

Where I is the current density, I_{st} is the stack current, A_{fc} is active cell area of the fuel cell

Activation losses:

$$V_{act} = a \ln \frac{I}{I_o}\ \ \mathrm{V} \quad (22)$$

where a and I_o are both constants determined experimentally.

Ohmic losses:

$$V_{ohm} = IR_{ohm} \text{ V} \quad (23)$$

$$R_{ohm} = \frac{T_m}{\sigma_m} \ \Omega \quad (24)$$

Where T_m is the thickness of the membrane and σ_m is the conductivity of the membrane.

$$\sigma_m = B_1 e^{\left(B_2\left(\frac{1}{303}-\frac{1}{T_{fc}}\right)\right)} \text{ S/m} \quad (25)$$

where T_{fc} is the operating temperature of the fuel cell.

$$B_1 = B_{11}\lambda_m - B_{12} \quad (26)$$

where B_{11}, B_{12}, and B_2 are constants determined experimentally.

Concentration losses:

$$V_{conc} = I(C_2 \frac{I}{I_{max}})^{C_3} \text{ V} \quad (27)$$

Where C_2, C_3, I_{max} are constants determined experimentally.

$$V_{fc}(\text{k}\Delta\text{t}) = \text{E}(\text{k}\Delta\text{t}) - V_{act}(\text{k}\Delta\text{t}) - V_{ohm}(\text{k}\Delta\text{t}) - V_{conc}(\text{k}\Delta\text{t}) \ \forall k \quad \text{V} \quad (28)$$

Where E is the open circuit voltage. Taking into account all the losses involved in the fuel cell, the output voltage can found using equation (28).

$$V_{fc_{total}} = nV_{fc}(\text{k}\Delta\text{t}) \ \ \forall k \text{ V} \quad (29)$$

Where n is the number of cells in the fuel cell.

$$P_{fc}(\text{k}\Delta\text{t}) = I_{fc}(\text{k}\Delta\text{t})V_{fc_{total}}(\text{k}\Delta\text{t})S_{FC}(\text{k}\Delta\text{t}) \ \forall k \text{ W} \quad (30)$$

The power provided by the super capacitor will be calculated using equation (30).

- **System Constraints**

$$ch_{B1}(\text{k}\Delta\text{t}) \leq S_{PV}(\text{k}\Delta\text{t}) \ \forall k \quad (31)$$

$$ch_{B2}(\text{k}\Delta\text{t}) \leq S_{PV}(\text{k}\Delta\text{t}) \ \forall k \quad (32)$$

Constraints (31) and (32) ensure that both batteries are only charged from the photovoltaic cell at time step k.

$$ch_C(\mathrm{k}\Delta\mathrm{t}) \leq S_{PV}(\mathrm{k}\Delta\mathrm{t})\ \forall k \quad (33)$$

Constraint (33) ensures that the super capacitor can only be charged from photovoltaic cell at time step k.

$$P_{B1}(\mathrm{k}\Delta\mathrm{t})(1 - ch_{B1}(\mathrm{k}\Delta\mathrm{t})) + P_{B2}(\mathrm{k}\Delta\mathrm{t})(1 - ch_{B2}(\mathrm{k}\Delta\mathrm{t})) + P_C(\mathrm{k}\Delta\mathrm{t})(1 - ch_C(\mathrm{k}\Delta\mathrm{t})) + P_{PV}(\mathrm{k}\Delta\mathrm{t}) + P_{FC}(\mathrm{k}\Delta\mathrm{t}) \geq P_{demand}(\mathrm{k}\Delta\mathrm{t})\ \forall k \quad (34)$$

Constraint (34) ensures that enough power is supplied to meet the demand of the system at all times.

$$ch_C(\mathrm{k}\Delta\mathrm{t}) + ch_{Bi}(\mathrm{k}\Delta\mathrm{t}) \leq 1 \quad \forall k \quad (35)$$

Constraint (35) ensures the super capacitor cannot be charged if any of the batteries is being charged.

3.5. Analytic Hierarchy Process (AHP)

An AHP will be used to calculate the weights used in the objective function. The criteria in which the sources will be evaluated on are: the cost of using the source, the ease of charging the source, the duration in which the source is able to supply power, and the discharge speed of the source.

The Analytic hierarchy process is a tool used for making complex decisions reducing them into a sequence of pairwise comparisons to help include both subjective and objective features of a decision. It is important to note that the best option of the alternatives is not one that is the most superior alternative at all criteria, rather it is the one that accomplishes the most appropriate tradeoff between the set of criteria.

For each criteria, a score is assigned to each of the alternatives according to the decision maker's pairwise comparisons of the alternatives regarding that specific criteria. The higher the score of the alternative, the better that alternative is with regards to that specific criteria. The scores used in the pairwise comparisons of the alternatives are shown in Table 1.

Table 1: AHP table of relative score [27]

VERBAL JUDGMENT OF PREFERENCE	NUMERICAL RATING
EXTREMELY PREFERRED	9
VERY STRONG TO EXTREMELY PREFERRED	8
VERY STRONGLY PREFERRED	7
STRONGLY TO VERY STRONGLY PREFERRED	6
STRONGLY PREFERRED	5
MODERATELY TO STRONGLY PREFERRED	4
MODERATELY PREFERRED	3
EQUALLY TO MODERATELY PREFERRED	2
EQUALLY PREFERRED	1

AHP also provides a weight for each of the evaluation criteria considered using the decision maker's pairwise comparisons of the criteria. The more important the criteria is to the decision makers, the higher the weight assigned to that criteria. The AHP then combines each of the alternative's scores with the weights of each criteria, to determine a global score for the alternatives. The global score for the alternatives is a weighted sum of the scores given to the alternative in reference to each of the criteria [27].

- **Cost of usage:**

Table 2 shows the relative scores of cost of usage for the different power sources. The cost of usage criteria refers to the cost incurred by the system each time the source is used to supply the demand of the system. Some of the costs a source could experience is the degradation that occurs to the source each time it is used or it could be the fuel used by the source, for instance the hydrogen used by fuel cells. Therefore, the cost of usage of the sources is as follows from most feasible to least feasible cost [28]:

1. Photovoltaic cell
2. Super capacitor
3. Fuel Cell
4. Battery

Table 2: Cost of usage relative scores.

COST OF USAGE					
SOURCE	**Battery**	**Fuel Cell**	**SC**	**PV**	**Average**
BATTERY	1	1/3	1/6	1/8	1/20
FUEL CELL	3	1	1/4	1/6	3/29
SC	6	4	1	1/3	19/68
PV	8	6	3	1	38/67

- **Ease of charge:**

Table 3 shows the relative scores for the different power sources. The ease of charge criteria refers to how easily a source can be charged during the flight of a drone. Some of the aspects considered were the duration needed to charge the source and by how many other sources can a source be charged by, for example the super capacitor can be charged by the batteries or the PV panel but the batteries can only be charged by the PV panel. Therefore, the ease of charge of the sources is as follows from highest to lowest [29]:

1. Super capacitor
2. Battery
3. Fuel Cell
4. Photovoltaic cell

Table 3: Ease of charge relative scores.

EASE OF CHARGE					
SOURCE	**Battery**	**Fuel Cell**	**SC**	**PV**	**Average**
BATTERY	1	4	1/2	8	9/28
FUEL CELL	1/4	1	1/5	7	10/71
SC	2	5	1	9	1/2
PV	1/8	1/7	1/9	1	1/26

- **Duration:**

Table 4 shows the duration relative scores for the different power sources. The duration criteria refers to how long the source can supply power to help meet the demand of the system before needing to be charged. Therefore, the duration of the sources from the highest duration to the lowest is as follows [30]:

1. Battery
2. Fuel cell
3. Photovoltaic cell
4. Super capacitor

Table 4: Duration relative scores.

DURATION					
SOURCE	**Battery**	**Fuel Cell**	**SC**	**PV**	**Average**
BATTERY	1	3	8	6	31/56
FUEL CELL	1/3	1	7	5	13/43
SC	1/8	1/7	1	1/3	1/21
PV	1/6	15	3	1	3/31

- **Discharge Speed:**

Table 5 shows the discharge speed relative scores for the different power sources. The discharge speed criteria refers to how quick the source can react and discharge to meet the demand of the system once given the command. Therefore, the discharge speed of the sources from the highest to the lowest is as follows [6, 29, 30]:

1. Super capacitor
2. Battery
3. Fuel Cell
4. Photovoltaic cell

Table 5: Discharge speed relative scores.

DISCHARGE SPEED					
SOURCE	**Battery**	**Fuel Cell**	**SC**	**PV**	**Average**
BATTERY	1	3	1/7	5	10/53
FUEL CELL	1/3	1	1/8	2	5/61
SC	7	8	1	9	19/28
PV	1/5	1/2	1/9	1	4/79

- **Criteria:**

Table 6 shows the criteria relative scores. The importance of each of the criteria will depend on the demand profile of the system. For instance, if the demand profile contains many spikes represents high wind speed then the discharge speed criteria will be given greater weight. This is done to make sure that the system can react in adequate time to the spikes of demand.

Table 6: Criteria relative scores

CRITERIA	COST OF USAGE	EASE OF CHARGE	DURATION	DISCHARGE SPEED	AVERAGE
COST OF USAGE	1	2	1/5	1/3	4/37
EASE OF CHARGE	1/2	1	1/7	1/5	1/16
DURATION	5	7	1	3	9/16
DISCHARGE SPEED	3	5	1/3	1	4/15

Finally, the ratings of each the alternatives is then multiplied by the weights of the sub-criteria and combined to get local ratings with respect to each of the criteria. The local ratings are then multiplied by the weights of the criteria and combined to get overall ratings of the alternatives.

Table 7: Weights assigned to each of the sources

WEIGHTS	
BATTERY	0.44
FUEL CELL	0.11
SC	0.20
PV	0.13

Chapter 4: Heuristic Approach

The developed model in Chapter 3 requires a long time to compute the optimal solution; therefore, a heuristic approach was developed to solve the problem under study with the objective of increasing the drone's flight distance and time. The heuristic approach identifies the smallest combination of sources needed to meet the demand of the system. A flow chart representing the heuristic algorithm is found in Appendix E. The heuristic algorithm used is as follows:

1: **for i=1:10**
2: **if** ($P_{demand}(i) > 200$)
3: **if** $P_{demand}(i) < P_{FC}$
4: $S_{FC}(i) = 1;$
5: **elseif** $P_{demand}(i) < P_{FC} + P_{PV}$
6: $S_{FC}(i) = 1;$
7: $S_{PV}(i) = 1;$
8: **elseif** $SOC_{B1}(i) > 47$
9: if $P_{demand}(i) < P_{FC} + P_{PV} + P_{B1}$
10: $S_{FC}(i) = 1;$
11: $S_{PV}(i) = 1;$
12: $S_{B1}(i) = 1;$
13: **elseif** $SOC_{B2}(i) > 47$
14: $S_{FC}(i) = 1;$
15: $S_{PV}(i) = 1;$
16: $S_{B1}(i) = 1;$
17: $S_{B2}(i) = 1;$
18: **elseif** $SOC_{C}(i) = 100$
19: $S_{FC}(i) = 1;$
20: $S_{PV}(i) = 1;$
21: $S_{B1}(i) = 1;$
22: $S_{C}(i) = 1;$
23: **end**
24: **elseif** $SOC_{B2}(i) > 47$
25: $S_{FC}(i) = 1;$
26: $S_{PV}(i) = 1;$
27: $S_{B2}(i) = 1;$
28: **elseif** $SOC_{C}(i) = 100$
29: $S_{FC}(i) = 1;$
30: $S_{PV}(i) = 1;$
31: $S_{B2}(i) = 1;$
32: $S_{C}(i) = 1;$
33: **end**
34: **end**
35: **if** $P_{demand}(i) \leq 200$
36: $S_{FC}(i) = 1;$

37: **if** $SOC_C(i) < 99$
38: $S_{PV}(i) = 1;$
39: $ch_c(i) = 1;$
40: **elseif** $SOC_{B1}(i) < 100$
41: $S_{PV}(i) = 1;$
42: $ch_{B1}(i) = 1;$
43: **elseif** $SOC_{B2}(i) < 100$
44: $S_{PV}(i) = 1;$
45: $ch_{B2}(i) = 1;$
46: **end**
47: **end for**
48: **return** $S_{FC}(i), S_{PV}(i), S_{B1}(i), S_{B2}(i), S_C(i), ch_C(i), ch_{B1}(i), ch_{B2}(i)$

The Heuristic algorithm starts with checking if the demand of power is greater than 200 W. The value of 200 W was chosen because the fuel cell provides 210 W of power at rated conditions. If the demand for power is less than or equal to 200 W, the system will move into a charging mode. The system will turn on the fuel cell to meet the demand of the drone and check if there is an output from the photovoltaic cell. If the photovoltaic cell is providing an output, the system will check whether or not the super capacitor is fully charged. If the super capacitor is not fully charged, the photovoltaic cell will charge it. Next, the system will check if the batteries are fully charged and if not they will be charged by the photovoltaic cell individually. On the other hand, if the photovoltaic cell does not provide an output the system will take no action and move to the next time instant.

If the demand for power is greater than 200 W, the system will move to supplying mode. First, the system will next check if there is a spike in the demand. A spike in demand is considered when the demand increases by 30% from one time instance to the next. This is done so that the system can discharge the super capacitor during spikes in demand due to the super capacitor's rapid discharge speed [25]. If there is a spike in power demand and the super capacitor is charged, the system will discharge the super capacitor along with other sources to meet the demand of the system. On the other hand, if there is no spike in demand the system will not discharge the super capacitor. Next, the system will check if there is an output from the photovoltaic cell to make use of the photovoltaic cell while it provides an output. Assuming that the photovoltaic cell is providing an output, the system will check which combination of sources along with the photovoltaic cell will be able to meet the demand of the system. For instance if the photovoltaic cell and fuel cell are not enough to meet the demand,

the system will first check the state-of-charge of the first battery. If the state-of-charge of the battery is between 47% and 100% the system will use the fuel cell, photovoltaic cell, and battery to meet the demand of the drone. If the state-of-charge of the first battery is less than 47%, the system will move to check the state-of-charge of the second battery and so on. The range of 47% to 100% was chosen because using a battery for one time instance reduces the state-of-charge of the battery by 17%. Therefore to keep the state-of-charge of the battery greater than or equal to 30%, a lower bound of 47% was chosen for the range. On the occasion that there is no output from the photovoltaic cell, the system will check the remaining sources to meet the demand on the system. Moreover, the heuristic algorithm could generate a solution in a matter of seconds on Matlab, while the dynamic algorithm used on Lingo required sometimes hours.

Chapter 5: Demonstration Examples and Results

The objective of this research is to generate an optimal switching sequence between the energy sources of the drone using the model discussed in chapter 3. In this section we will review simulations conducted for different scenarios that the drone is likely to encounter. The scenarios reviewed in Sections 5.1-5.4 include: object pickup, altitude maintenance, multiple object pickup, and extreme conditions. Additionally, Sections 5.5 and 5.6 include sensitivity analysis of the performance of the model in cases where the batteries are initially not fully charged and the rating of the photovoltaic cell is reduced. The following simulations were conducted on Lingo to obtain an optimal solution to the model as well as on Matlab for a heuristic approach and a standard mode of operation. The standard mode of operation considered represents using each source separately until the source is completely depleted; starting with the first battery, followed by the second battery, super capacitor, fuel cell, and finally the photovoltaic cell. The algorithms used on Lingo and Matlab are found in Appendix A and B respectively in addition to further sensitivity analysis in Appendix C. Additionally, the simulations were conducted for ten time steps where the step size is five seconds. Only ten time steps were considered due to the large computing power needed to conduct simulations for the full length of a drone's flight.

5.1. Illustrative Example 1: Object Pickup

The following simulation represents the situation were a drone must travel to a certain location to pick up an object and return the object to the drone's base. During this simulation, ideal conditions are considered were the drone does not face any distribution or turbulence during its flight. The demand profile of this simulation is shown in Figure 5, initially the drone starts traveling to the location where the object is located. At time step 4, the drone reaches the object's location and descends to pick up the desired object. After the drone picks up the object, it continues its flight to return to its base.

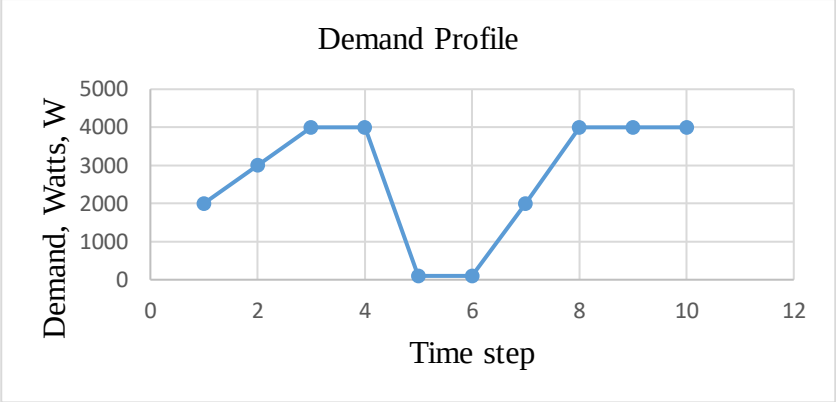

Figure 5: Demand profile for simulation 1

System voltages:

Figures 6 and 7 display the system voltages for both the dynamic approach and heuristic approach respectively. In this example, the switching sequence generated by the dynamic approach chose not to use the super capacitor while the heuristic approach did.

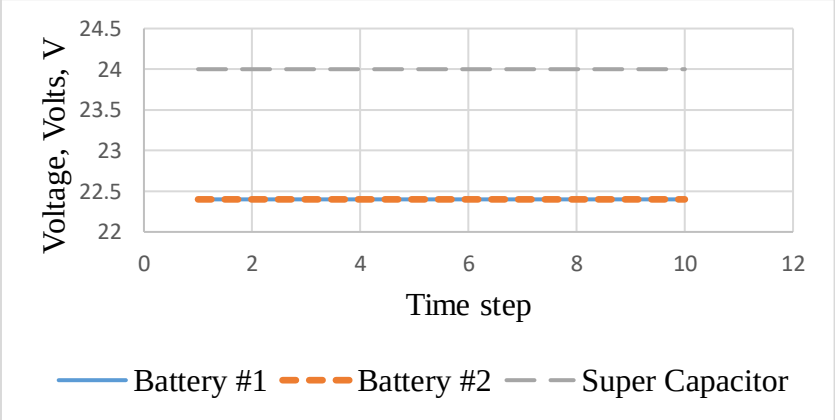

Figure 6: Dynamic approach voltages

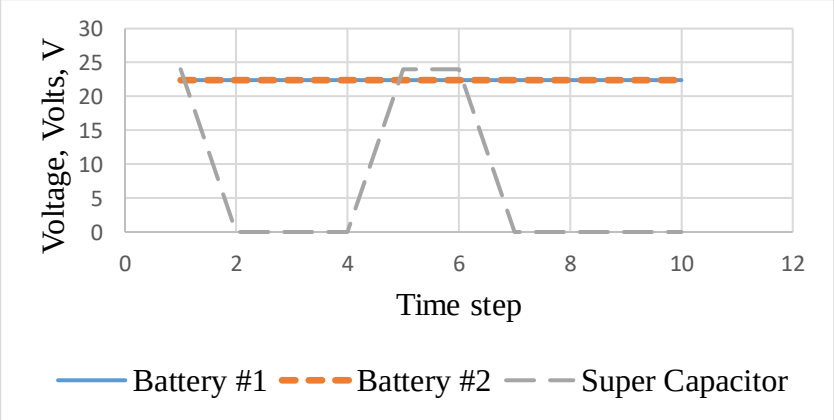

Figure 7: Heuristic approach voltages

System currents:

Figures 8 and 9 display the system currents for both the dynamic approach and heuristic approach respectively. As the super capacitor was not used by the dynamic approach, the current remains 0 while the currents of the batteries vary as they are being used. However, in the heuristic approach both batteries and the super capacitor were used therefore their currents vary accordingly.

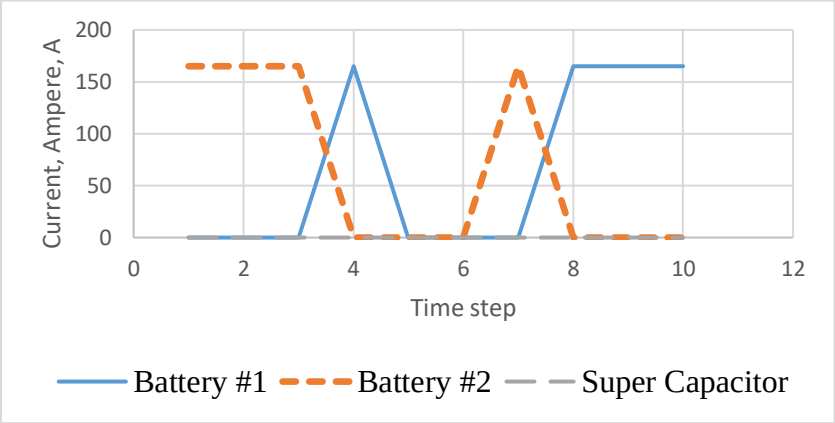

Figure 8: Dynamic approach currents

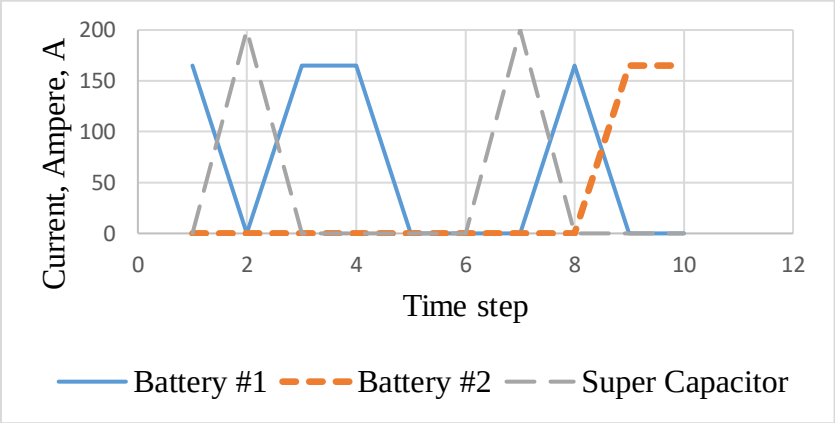

Figure 9: Heuristic approach currents

System state-of-charge:

Figures 10 and 11 display the changes in the state-of-charges of the batteries and super capacitor for both the dynamic approach and heuristic approach.

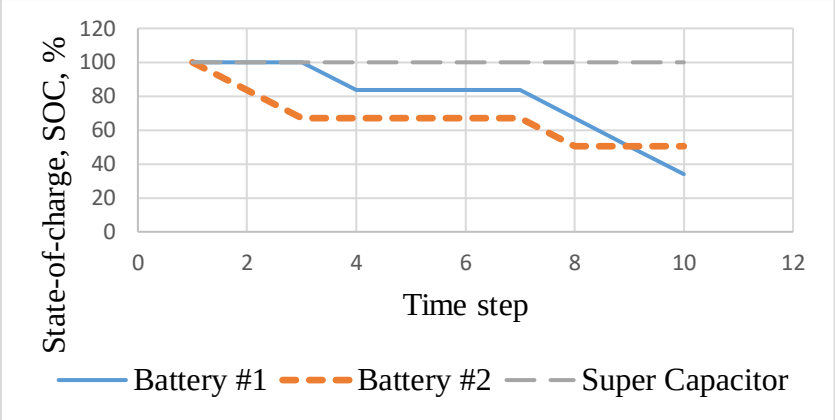

Figure 10: Dynamic approach state-of-charges

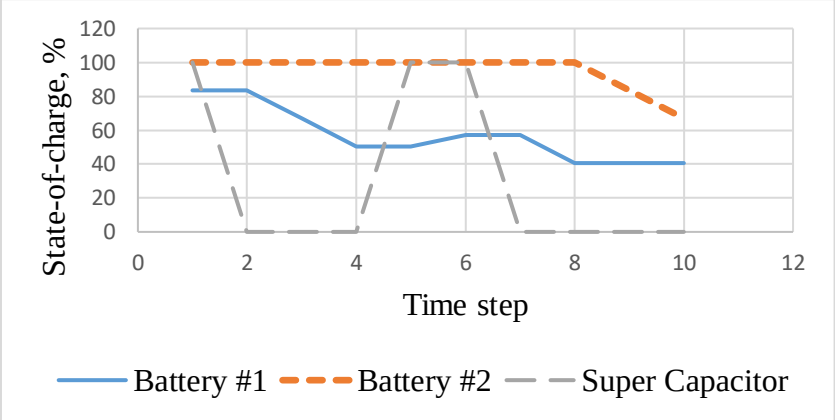

Figure 11: Heuristic approach state-of-charges

System power consumption:

In the object pickup simulation, both the switching sequences of the dynamic approach and heuristic approach were able to meet the demand of the drone but that of the standard approach did not. After both batteries and super capacitor were completely depleted, the standard approach was unable to meet the demand of the drone in the 10^{th} time instance. However although both the switching sequences of dynamic approach and heuristic approach met the demand, the dynamic approach provided a sequence of switching superior to that of the heuristic approach. The obtained objective function value of the dynamic approach was 9% lower with a value of 6536.2, while the heuristic approach's was 7123.3. However, the switching sequences of the heuristic approach had a lower average power consumption of 3361.2 W compared to the dynamic approach's 3720 W. This is due to the switching sequence of the dynamic approach resulting in significantly power consumption in time steps 6 and 7. The power used to meet the demand of the drone during each time step is shown in Figure 12. In addition,

the switching sequences generated by both the dynamic approach and heuristic approach are found in Appendix D.

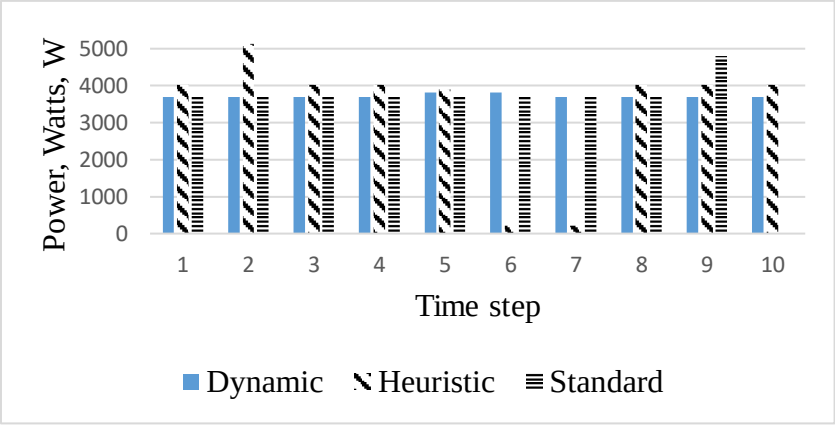

Figure 12: Power consumption comparison

5.2. Illustrative Example 2: Altitude Maintenance

The following simulation represents the situation were a drone must maintain a certain height above the ground for a short period of time. During its flight, the drone faces turbulence causing fluctuations in the demand profile. The demand profile of this simulation is shown in Figure 13; the drone starts ascending to the required height thus causing an increased in the demand of the drone. At time step 3, the drone reaches the required height and tries maintains it for 5 time steps. However, the drone faces significant turbulence causing fluctuations in the height it maintains which is represented in the demand profile. Finally, the drone begins to descend back to its base.

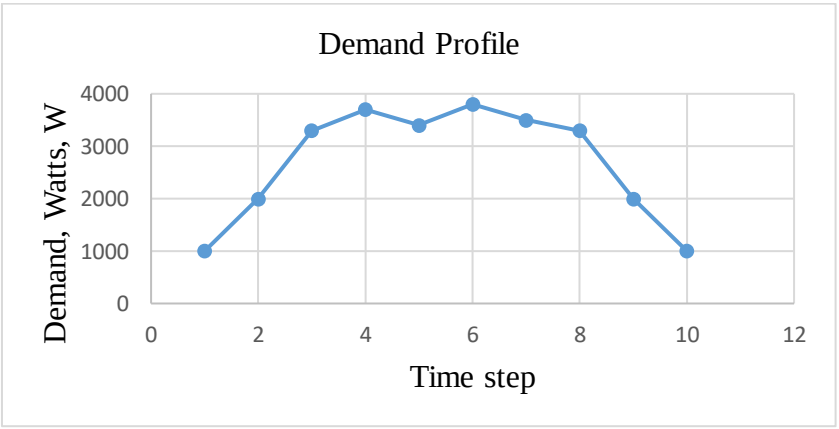

Figure 13: Demand profile for simulation 2

System voltages:

Figures 14 and 15 display the system voltages for both the dynamic approach and heuristic approach respectively. Also in this example, the switching sequence

generated by the dynamic approach chose not to use the super capacitor while the heuristic approach did.

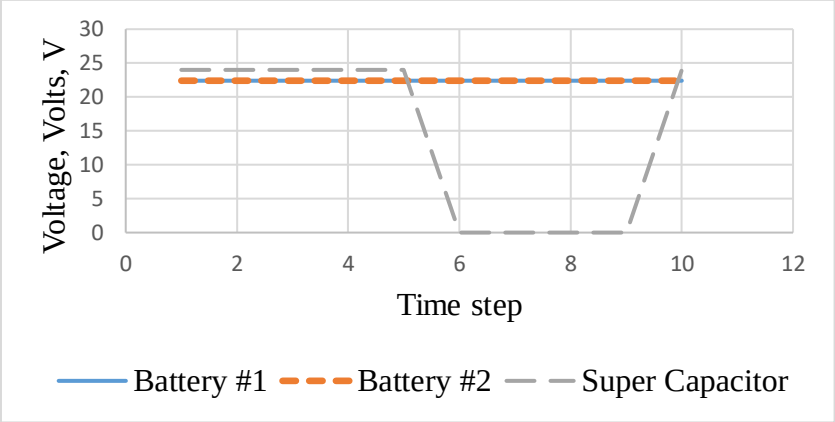

Figure 14: Dynamic approach voltages

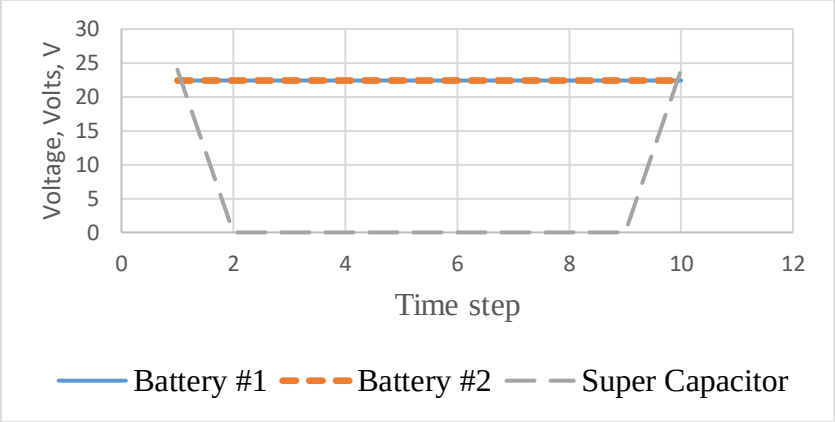

Figure 15: Heuristic approach voltages

System currents:

Figures 16 and 17 display the system currents for both the dynamic approach and heuristic approach respectively. As the super capacitor was not used by the dynamic approach, the current remains 0 while the currents of the batteries vary as they are being used. However, in the heuristic approach both batteries and the super capacitor were used therefore their currents vary accordingly.

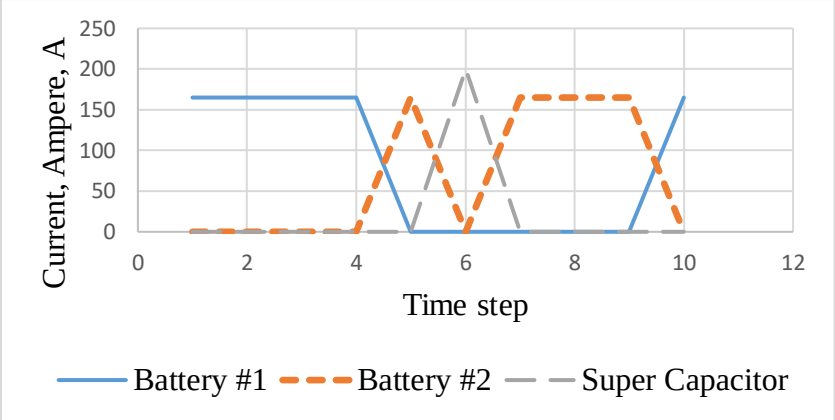

Figure 16: Dynamic approach currents

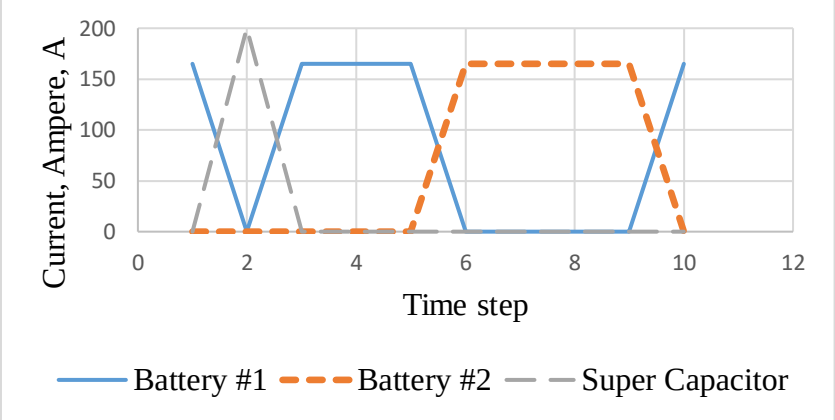

Figure 17: Heuristic approach currents

System state-of charges:

Figures 18 and 19 display the change in the state-of-charges of the batteries and super capacitor for both the dynamic and heuristic approach.

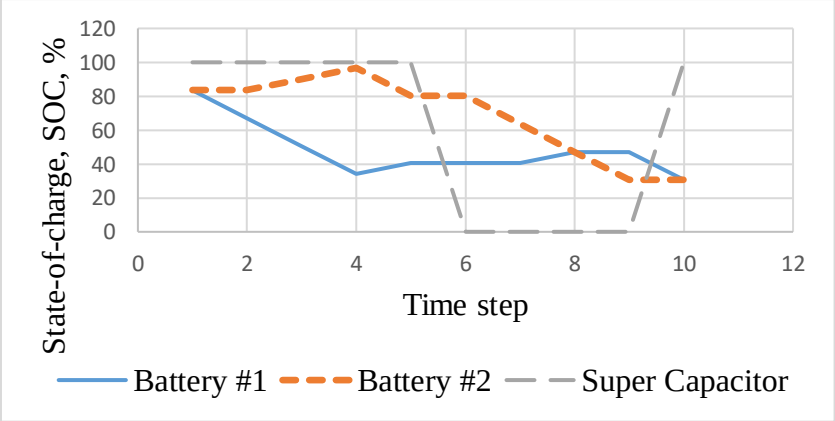

Figure 18: Dynamic approach state-of-charges

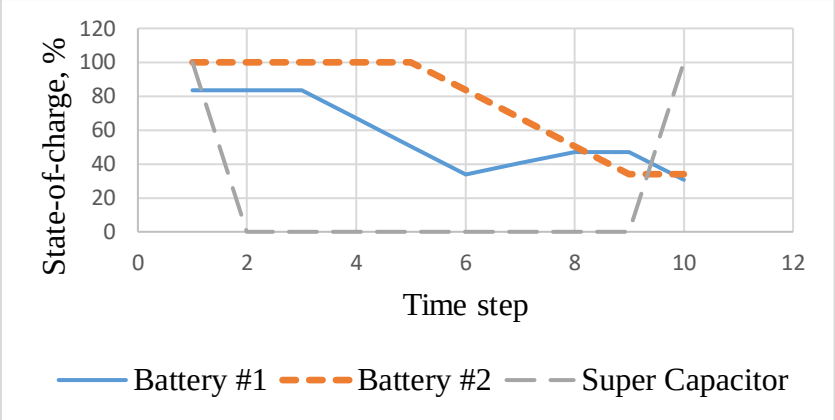

Figure 19: Heuristic approach state-of-charges

System power consumption:

In the altitude maintenance simulation, both the switching sequences of the dynamic and heuristic approach were able to meet the demand of the drone but that of the standard approach did not. While the drone was attempting to maintain the required altitude, the demand was higher than the power that the sources can provide separately. Therefore, resulting in the standard approach's inability to meet the demand of the drone. Additionally in this simulation, the dynamic approach performed better than the heuristic approach. The dynamic approach provided a sequence of switching between the sources that resulted in an objective function value of 8301.2, while the heuristic approach's was 8501.3. Additionally, the average power consumption obtained using the dynamic approach was 3827.4 W, while the heuristic approached resulted in 4136.4 W. The power used to meet the demand of the drone during each time step is shown in Figure 20. In addition, the switching sequence generated by both the dynamic and heuristic approach is found in Appendix D.

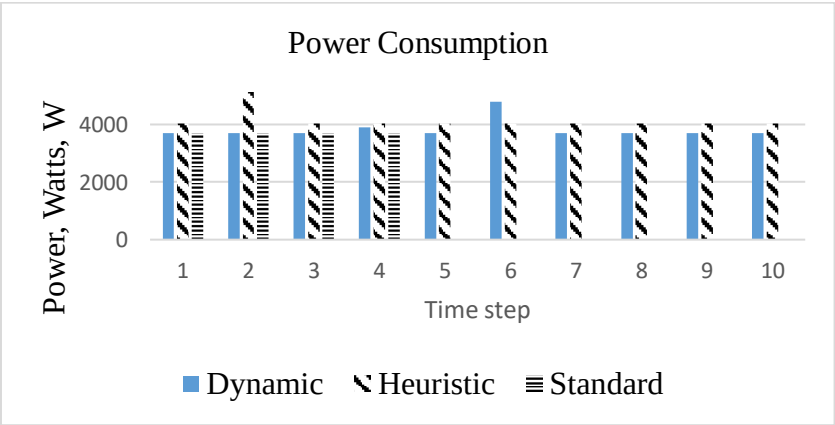

Figure 20: Power consumption comparison

5.3. Illustrative Example 3: Multiple object pickup

The following simulation represents a drone conducting multiple pickups of objects located in close proximity to each other. The demand profile of this simulation is shown in Figure 21. The weights assigned to the sources in the objective function have be manipulated to account for the multiple spikes of demand during the drone's flight. As shown in the demand profile, the drone starts traveling to the location where the first object is located. At time step 2, the drone reaches the object's location and descends to pick up the object. After the drone picks up the object, it continues to proceed to pick up the next object until all four objects are obtained. As the drone picks up each object the demand increases, as the load carried by the drone increases.

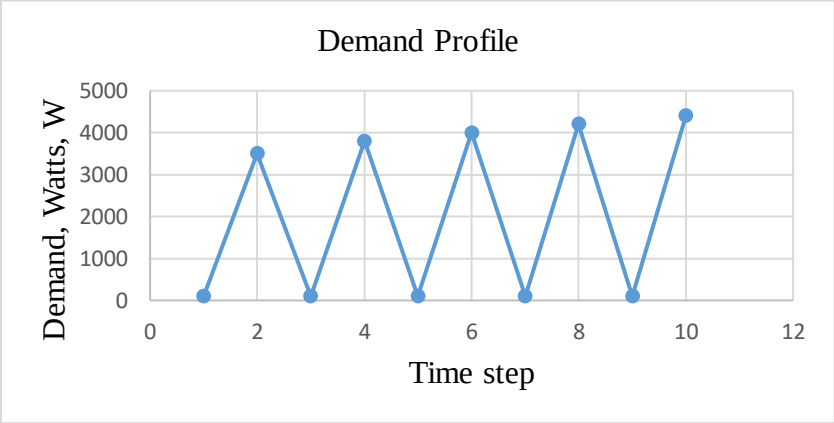

Figure 21: Demand Profile for simulation 3

System voltages:

Figures 22 and 23 display the system voltages for both the dynamic and heuristic approach respectively. In this example, the switching sequence generated by the dynamic approach chose to mainly use the super capacitor as did the heuristic approach to meet the demand of the drone.

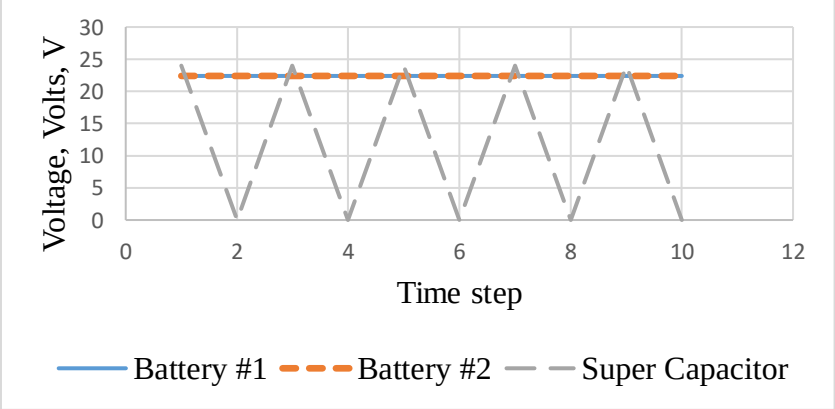

Figure 22: Dynamic approach voltages

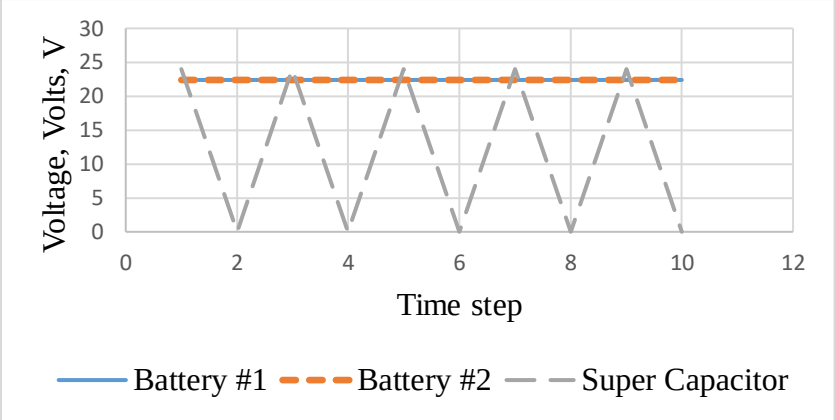

Figure 23: Heuristic approach voltages

System currents:

Figures 24 and 25 display the system currents for both the dynamic and heuristic approach respectively. As the super capacitor was mainly used by both the dynamic and heuristic approach, the super capacitor's current varies in a similar manner to that of the drone's demand.

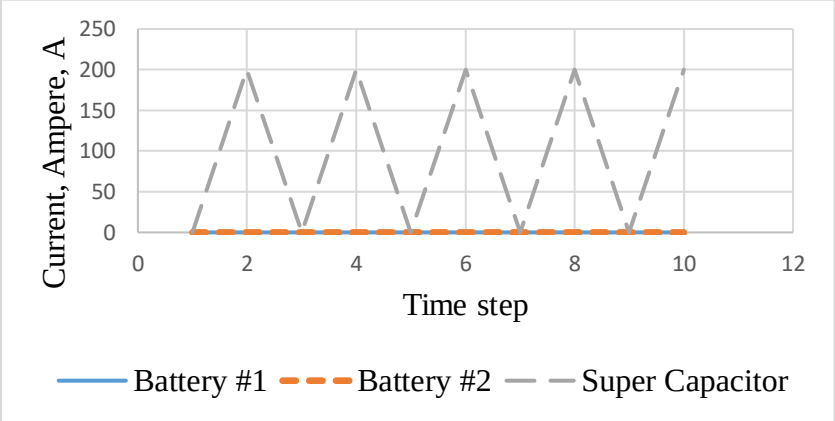

Figure 24: Dynamic approach currents

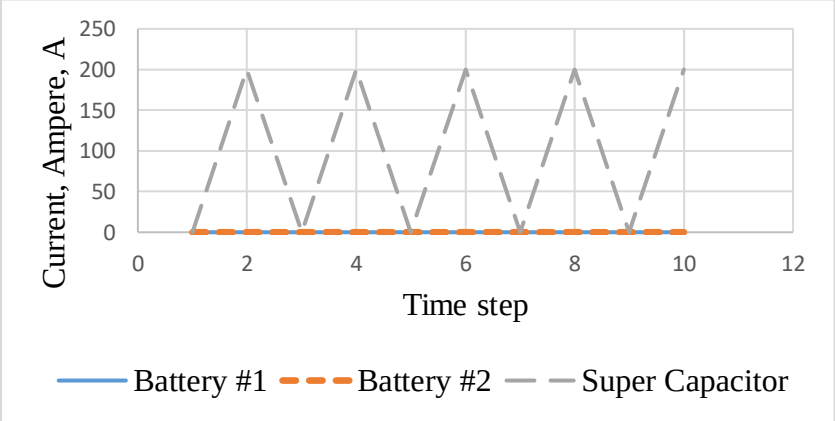

Figure 25: Heuristic approach currents

System state of charges:

Figures 26 and 27 display the change in the state-of-charges of the batteries and super capacitor for both the dynamic and heuristic approach. Since the batteries were not using in this example, the state-of-charge of the batteries remains 100% while the super capacitor is charged and discharge multiple times to meet the demand.

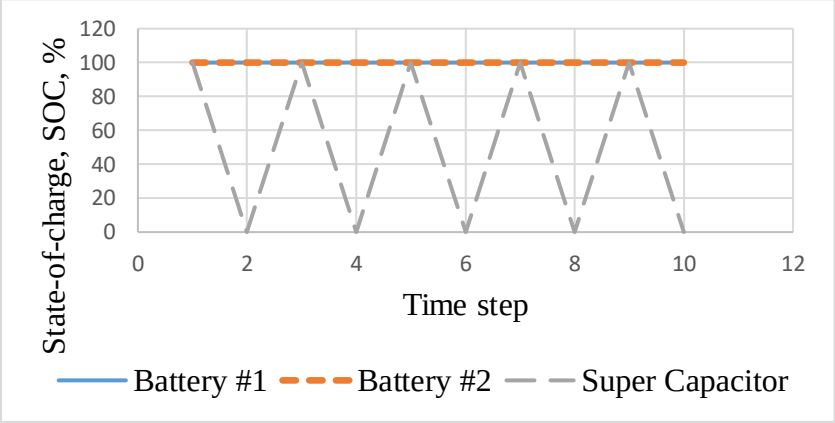

Figure 26: Dynamic approach state-of-charges

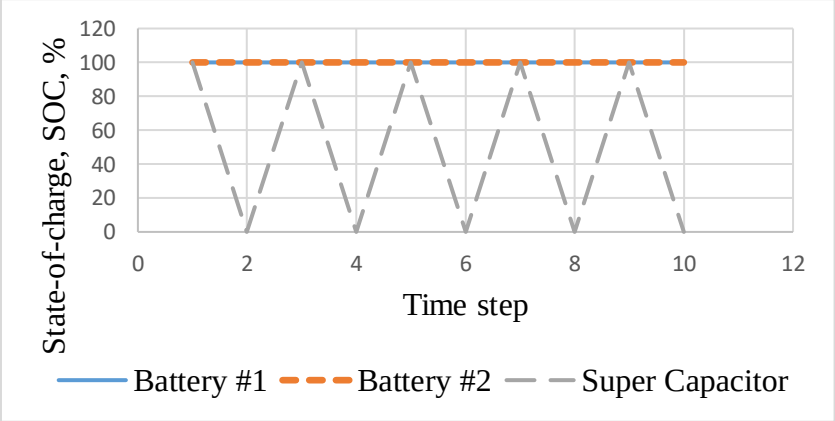

Figure 27: Heuristic approach state-of-charges

System power consumption:

In the multiple object pickup simulation, both the switching sequences of the dynamic and heuristic approach were able to meet the demand of the drone but that of the standard approach did not. The switching sequences of the standard approach was unable to meet the demand of the drone due to the multiple spikes in the demand. During spikes in demand, the use of the super capacitor is preferred due to its rapid discharge rate making it best equipped to handle spikes. The switching sequences of the dynamic and heuristic approach both utilized the super capacitor to meet the spikes

in demand of the drone. Additionally in both the super capacitor was charged when the demand was low so that it could be used during the next spike in demand. However although both the methods performed in a similar manner, the dynamic approach chose to use the photovoltaic cell in the first time step rather than the fuel cell to meet the demand. Therefore, resulting in an objective function value of 3499.2 and average power consumption of 2496 W for the switching sequence of the dynamic approach. On the other hand, the switching sequence of the heuristic approach resulted in an objective function value of 3517.5 and average power consumption of 2505 W. Therefore, resulting in a slightly lower power consumption which is shown in Figure 28. In addition, the switching sequence generated by both the dynamic and heuristic approach is found in Appendix D.

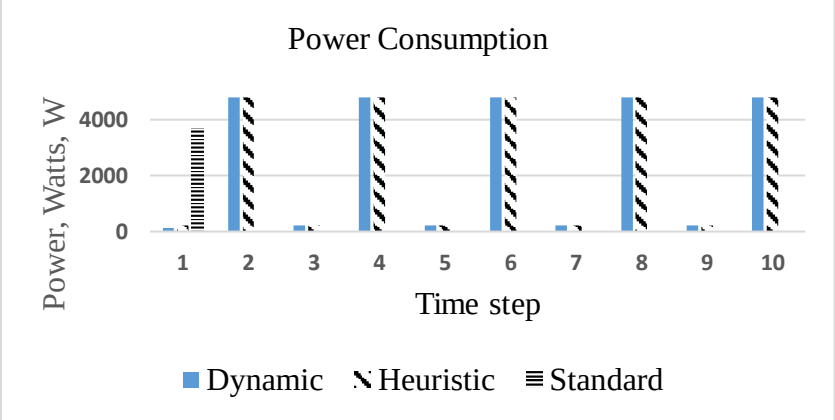

Figure 28: Power consumption comparison

5.4. Illustrative Example 4: Extreme conditions

The following simulation represents a drone facing extreme conditions where all sources, except the super capacitor, are completely depleted and the drone is unable to return to the base. The simulation was conducted for 3 time steps, in which the system was required to send a distress signal containing the drone's location to its base in order to be retrieved. The demand profile of this simulation is shown in Figure 29. As shown in the demand profile, the demand is initially zero and starts increasing as the drone is preparing to send the distress signal to its base.

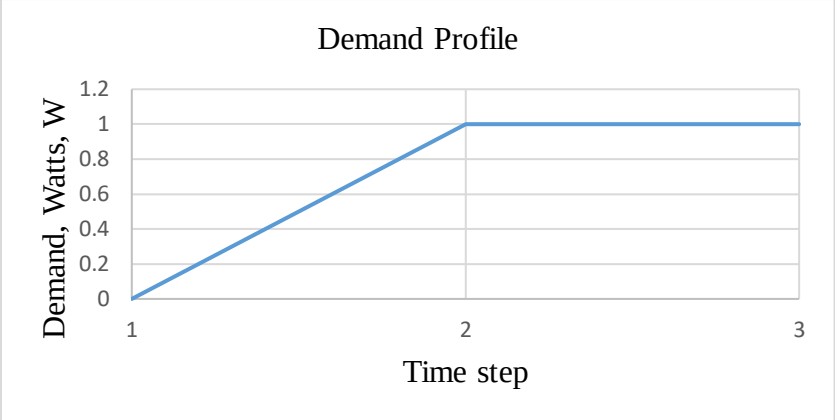

Figure 29: Demand profile for simulation 4

System Response:

Figure 30 shows the system voltages for the dynamic programming. As shown, the voltage of super capacitor drops to 0 after the super capacitor was used to charge the first battery.

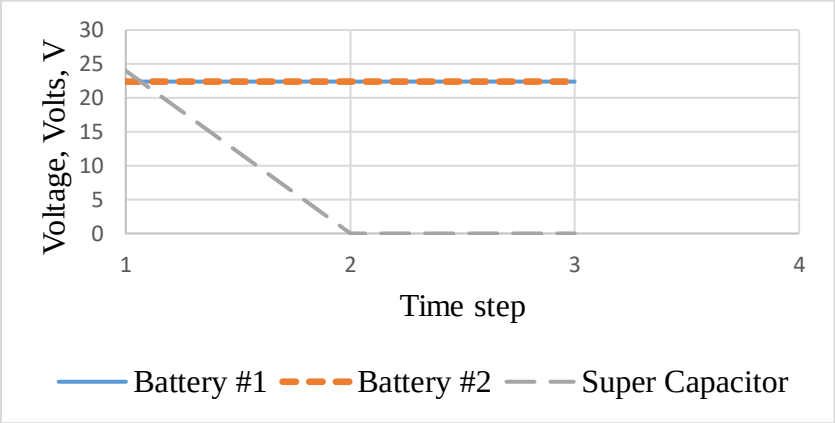

Figure 30: Extreme conditions system voltages

Figure 31 shows the system currents for the dynamic approach.

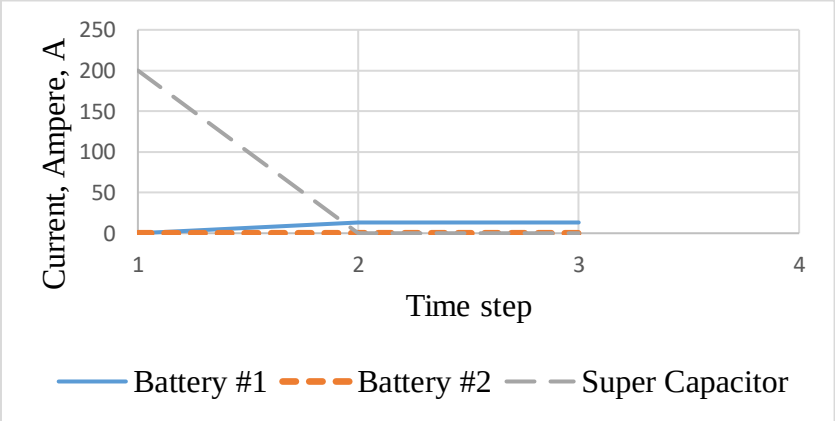

Figure 31: Extreme conditions system currents

Figure 32 shows the system state-of-charges for the dynamic approach. Initially, the super capacitor was fully charge and both batteries had a state-of-charge of 30%. In the first time step, the super capacitor was used to charge the first battery thus increase the first battery's state-of-charge to 46.5%.

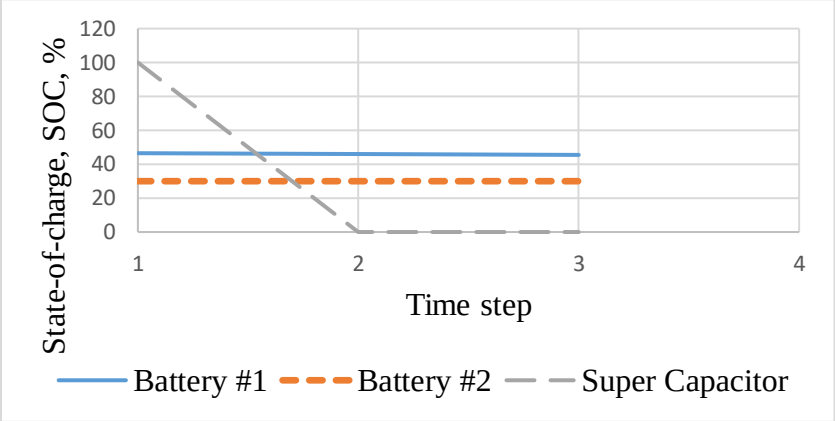

Figure 32: Extreme conditions system state-of-charges

In the extreme conditions simulation, the system was required to generate an optimal switching sequence between the sources to meet the demand of the drone to send a distress signal to the base. The obtained switching sequence resulted in using the super capacitor to charge the first battery in the first time step. Having charged the battery, the system assigned using the first battery to meet the demand of the drone and send a distress signal to the base as shown in Figures 30-32. The battery will continue to send a single to the base containing the drone's location until the drone is successfully retrieved.

5.5. Sensitivity Analysis

5.5.1. Object pickup with batteries initially not fully charged. The following simulation is similar to the first object pickup simulation in section 5.1 where a drone must travel to a certain location to pick up an object and return the object to the drone's base. However, in this simulation the batteries are not initially fully charged. The state-of-charge of the first battery is 80% and the state-of-charge of the second battery is 50%. The demand profile for this simulation is shown in Figure 33.

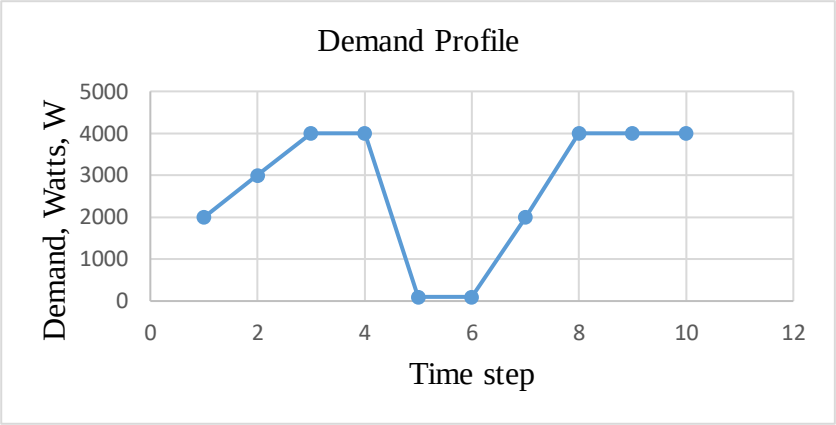

Figure 33: Demand profile for simulation 5

System Response:

Figure 34 shows the system voltages for the dynamic approach. As shown, the super capacitor is used twice along with the batteries to meet the demand of the drone.

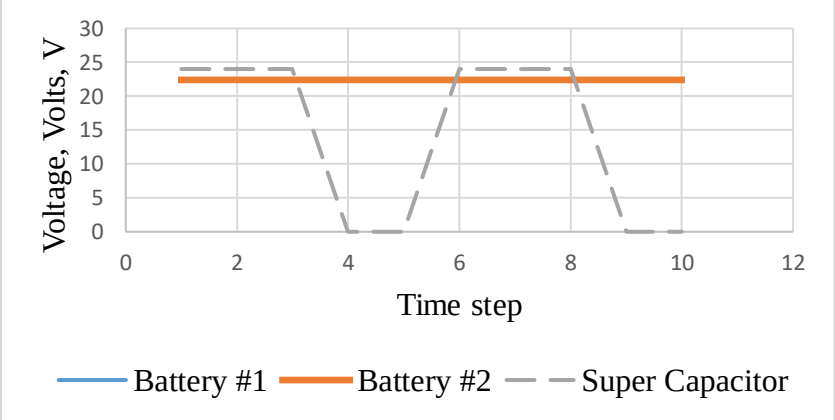

Figure 34: System voltages for simulation 5

Figure 35 shows the system currents corresponding the switching algorithm generated by the dynamic approach.

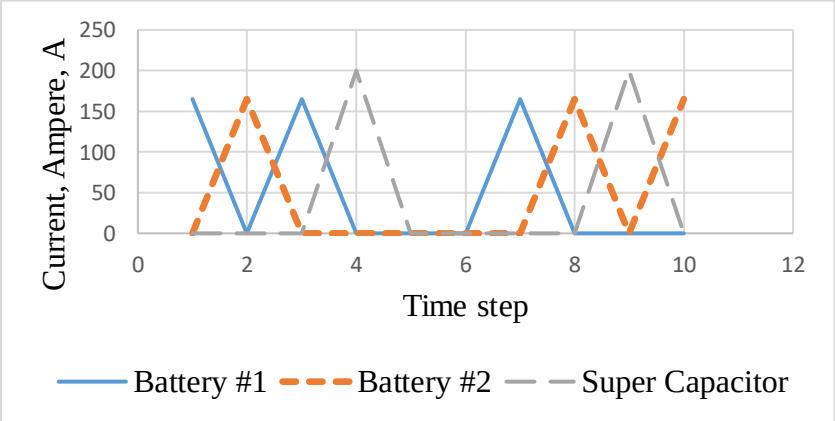

Figure 35: System currents for simulation 5

Figure 36 shows the system state-of-charges for the dynamic approach.

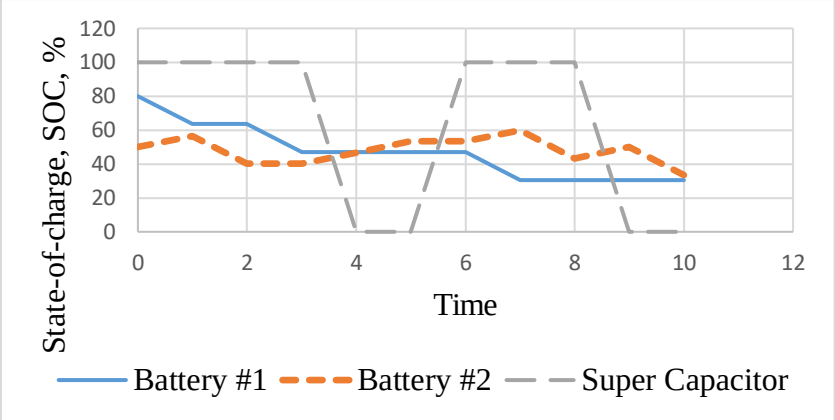

Figure 36: System state-of-charges for simulation 5

System power consumption:

In the object pickup simulation with the first battery and second battery initially charged at 80% and 50% respectively, only the switching sequence of the dynamic approach was able to meet the demand of the drone. The switching sequence of the standard approach failed after both batteries and super capacitor were completely depleted after the 5th time step. Similarly, the switching sequence of the heuristic approach failed after the 8th time step when the demand was too high for the system to charge either the batteries or the super capacitor to meet the demand in the 9thand 10th time step. Moreover, the dynamic approach generated a switching sequence that met the drone's demand with an objective function value of 6844.9 and average power consumption of 3219.6 W which is shown in Figure 37.

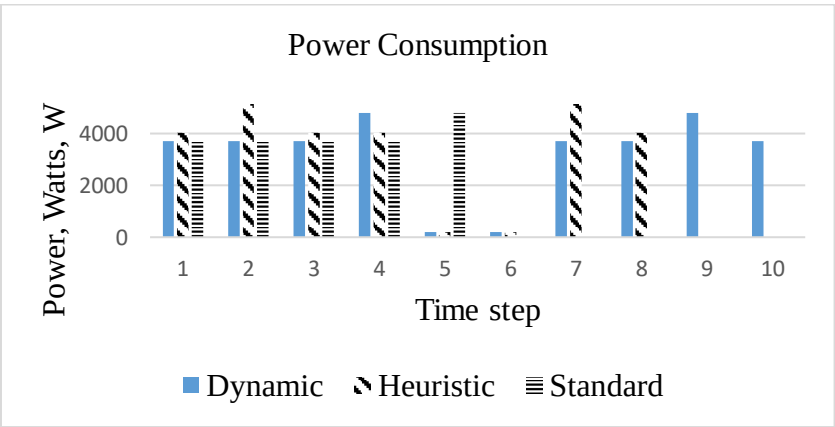

Figure 37: Power consumption comparison

5.5.2 Multiple altitude maintenance. The following simulation represents the situation where a drone must maintain several heights above the ground for a period of time with a lower rated photovoltaic cell of 80 W. A lower rating photovoltaic cell will result in charging the batteries 3.3% each time step, rather than 6.6% which was

achieved with the higher rating photovoltaic cell of 120 W in the previous simulations. The demand profile of this simulation is shown in Figure 38; the drone maintains the first required height till the 3rd time step. Next, the drone ascends to the second required height thus causing the demand to increase. Finally, the drone descends to the final required height and maintains it for 4 time steps.

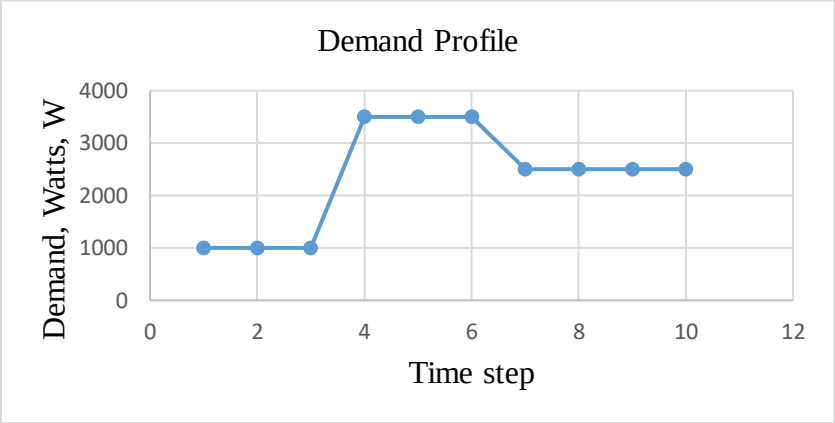

Figure 38: Demand profile for simulation 6

System Response:

Figure 39 shows the system voltages for the dynamic approach. As shown the super capacitor was only used once.

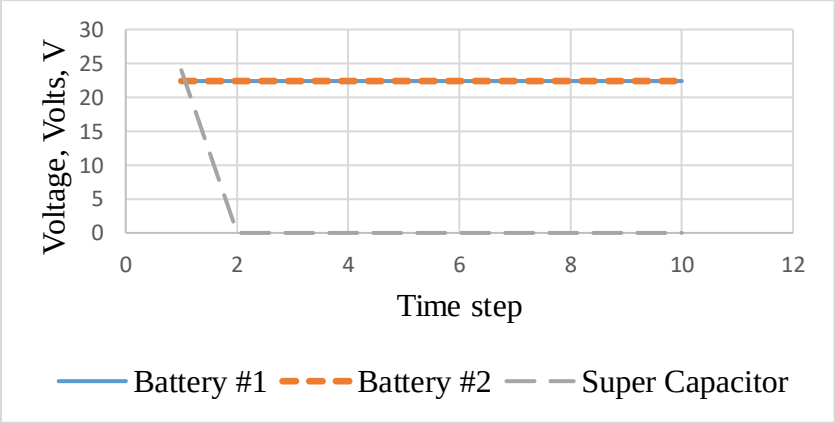

Figure 39: System voltages for simulation 6

Figure 40 shows the system currents corresponding the switching algorithm generated by the dynamic appraoch.

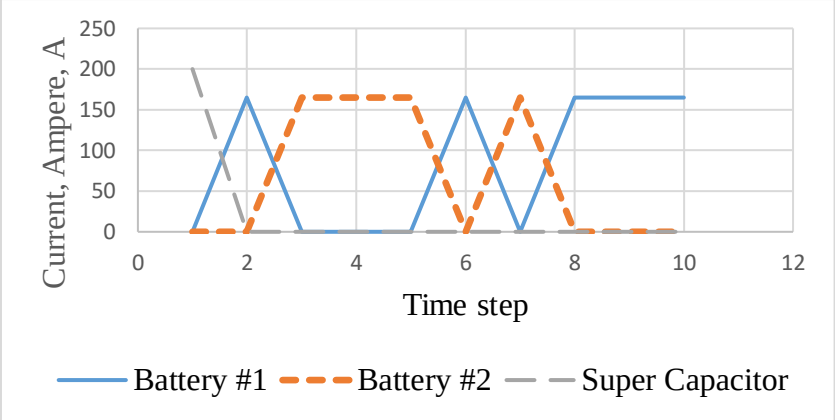

Figure 40: System currents for simulation 6

Figure 41 shows the system state-of-charges for the dynamic approach. As shown, the first battery was charged multiple times to meet the demand of the drone,

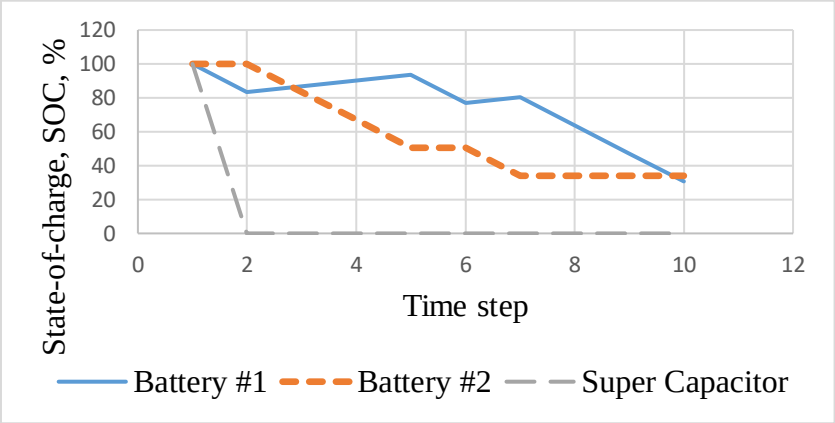

Figure 41: System state-of-charges for simulation 6

System power consumption:

In the multiple altitudes maintenance simulation, only the switching sequence of the dynamic approach was able to meet the demand of the drone. The switching sequence of the standard approach failed after both batteries and super capacitor were completely depleted after the 9th time step. Similarly, the switching sequence of the heuristic approach failed after the 9^{h} time step when the demand was too high for the system to charge either the batteries or the super capacitor to meet the demand in the 10th time step. Moreover, the dynamic approach generated a switching sequence that met the drone's demand with an objective function value of 7782.5 and average power consumption of 3806.4 W which is shown in Figure 42.

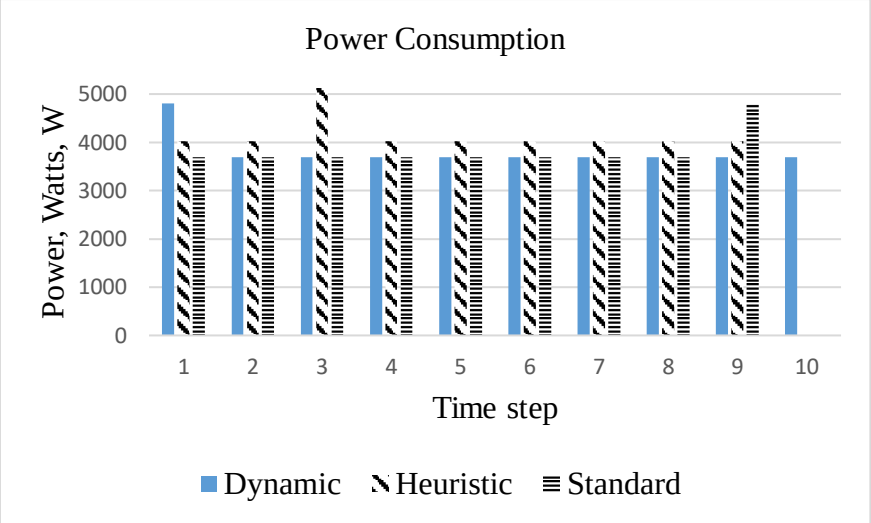

Figure 42: Power comparison for simulation 6

5.6. Experimental Work

The following experiment was conducted on a ground robot built at AUS, A picture of the ground robot is shown in Figure 43.

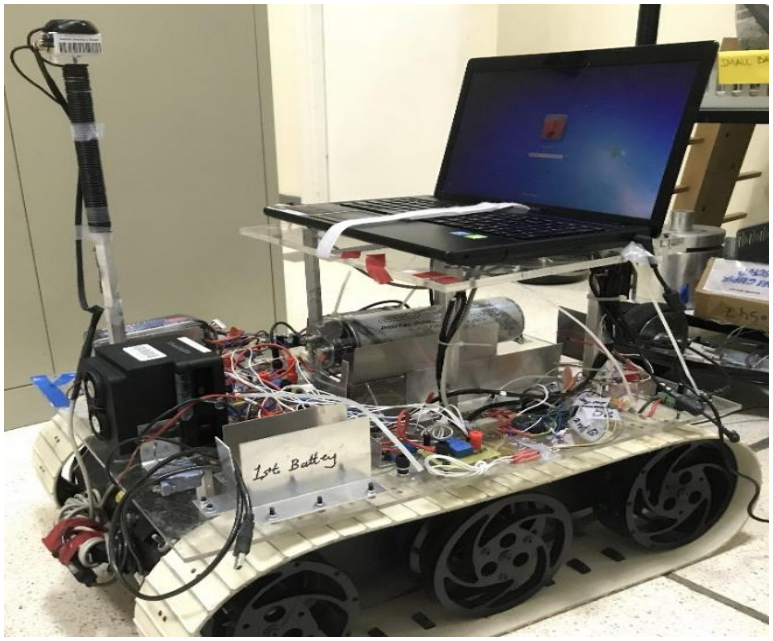

Figure 43: AUS ground robot built by Ali Al Tamimi

The ground robot contains three sources; a battery, super capacitor, and fuel cell. These sources are labeled in Figure 44.

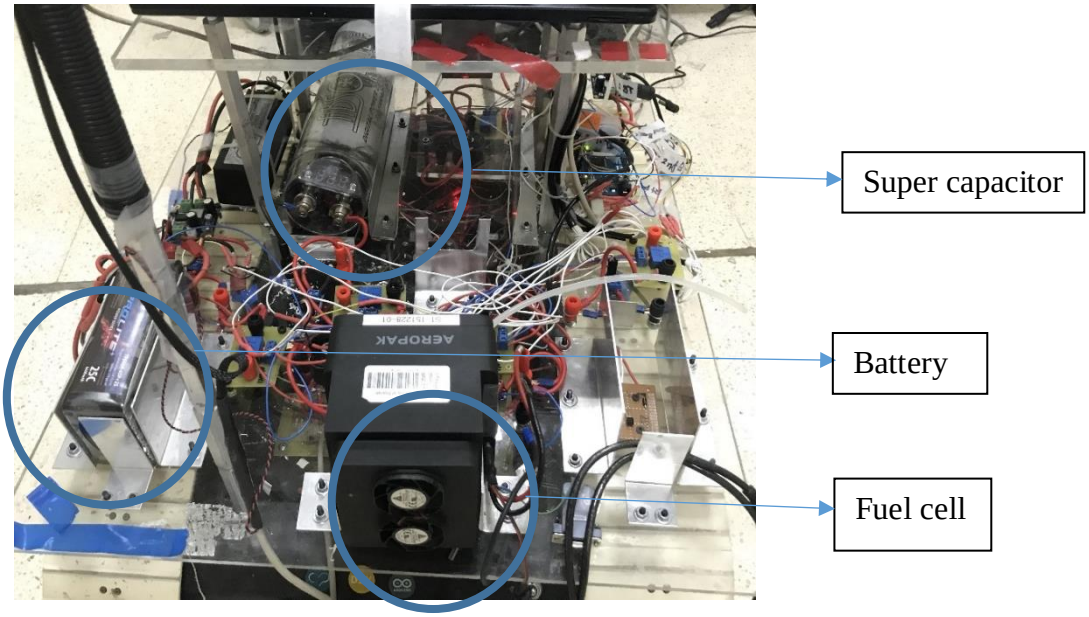

Figure 44: AUS ground robot sources

The robot was run in remote control mode while conducting the tests. The remote controller is shown in Figure 45.

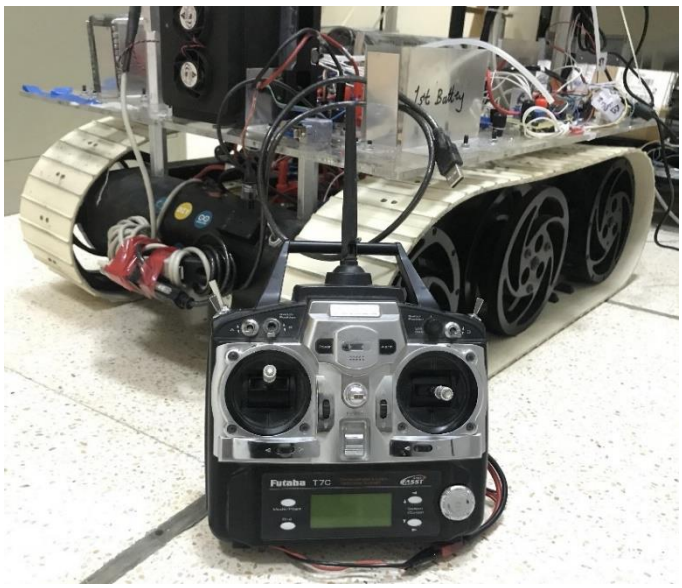

Figure 45: Ground robot remote controller

The robot was controlled by the remote controller to move around a lab bench in the Mechatronics lab in AUS. The lab bench is shown in Figure 46.

Figure 46: Table used for ground robot testing

By moving around the lab bench in the mechatronics lab, the ground robot was following a rectangular path of the dimensions shown in Figure 47.

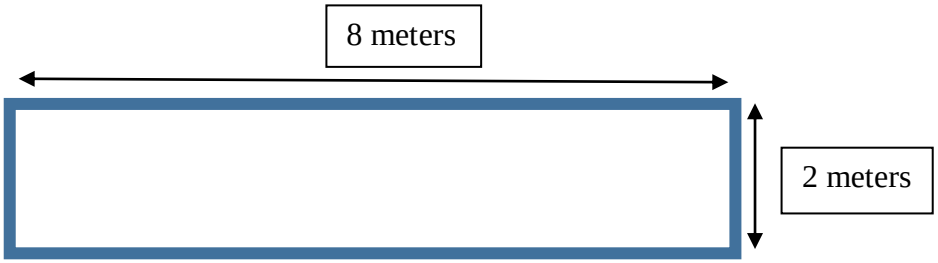

Figure 47: Path followed by the ground robot.

The demand profile for all tests is shown in figure 48.

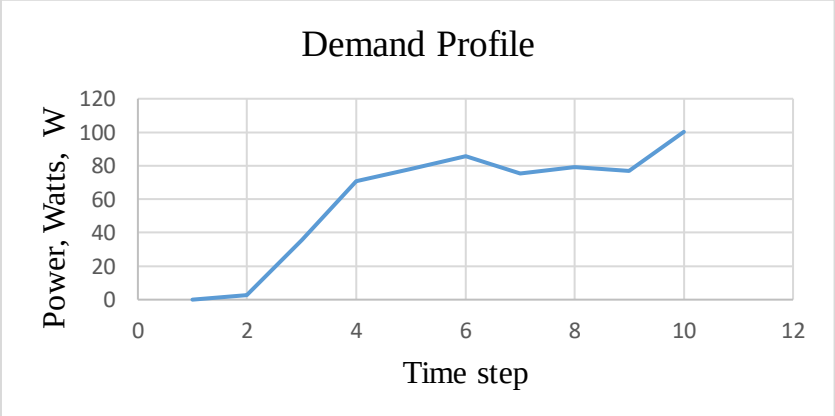

Figure 48: Demand profile for experimental work

The demand profile was uploaded to both the dynamic and heuristic algorithm to obtain a switching sequence. The ground robot has a controller which supplies a given amount of current to the motors if it is given a reference current. However, there is not necessarily a controller which controls where the current comes from. The switching sequences generated by the dynamic and heuristic approach tell this same lower level controller what sources to use to supply the required current; in order to satisfy the demand and still reduce the average power consumption across the sources. The switching sequences were then uploaded to the main controller of the ground robot, an Arduino microcontroller that controls the switches attached to the sources. After the switching sequence was uploaded, the ground robot performed a lap along the rectangular path. The power consumption across all sources after the ground robot completes a lap with the uploaded switching sequences was then compared with the standard mode of operation. For a ground robot, the standard mode of operation of the ground robot is using the battery to meet the demand until it's completely depleted then moving to the other available sources.

System voltages:

Figures 49, 50, and 51 display the system voltages for the standard mode, dynamic programming approach, and heuristic approach respectively. The standard mode of operation did not involve the super capacitor in meeting the demand of the ground robot, however the dynamic programming approach and heuristic approach did.

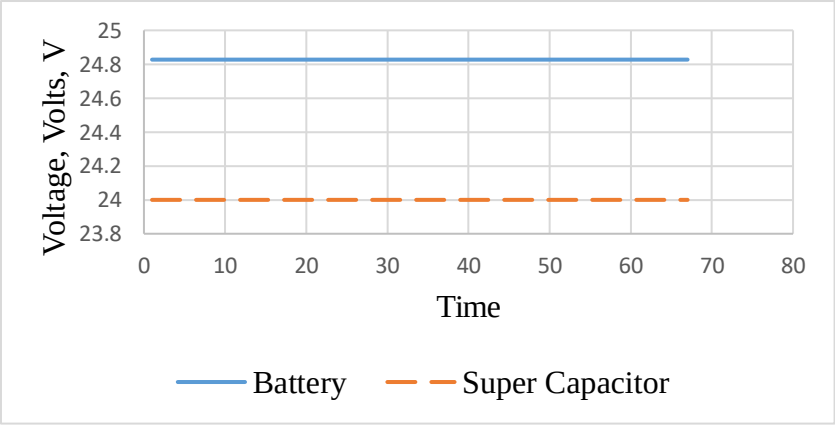

Figure 49: Standard mode system voltages

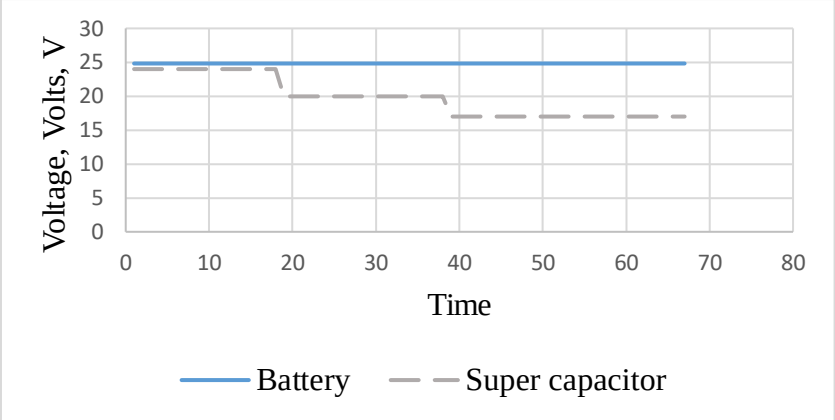

Figure 50: Dynamic approach system voltages

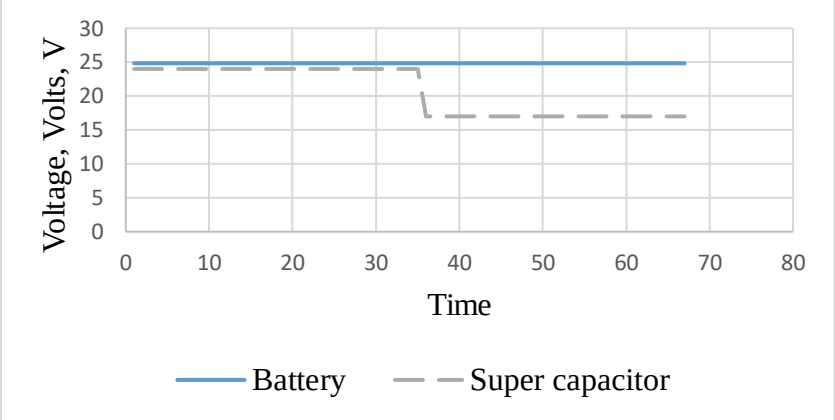

Figure 51: Heuristic approach system voltages

System currents:

Figures 52, 53, and 54 display the system currents for the standard mode, dynamic approach, and heuristic approach respectively. The use of the super capacitor by the dynamic programming approach and heuristic approach is apparent in Figures 54 and 55.

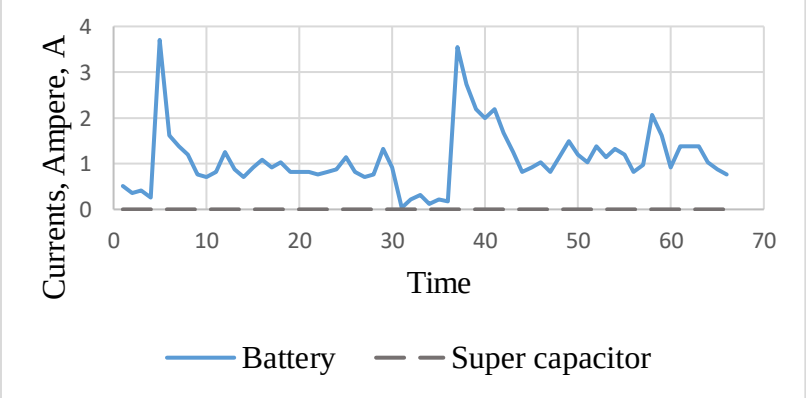

Figure 52: Standard mode system currents

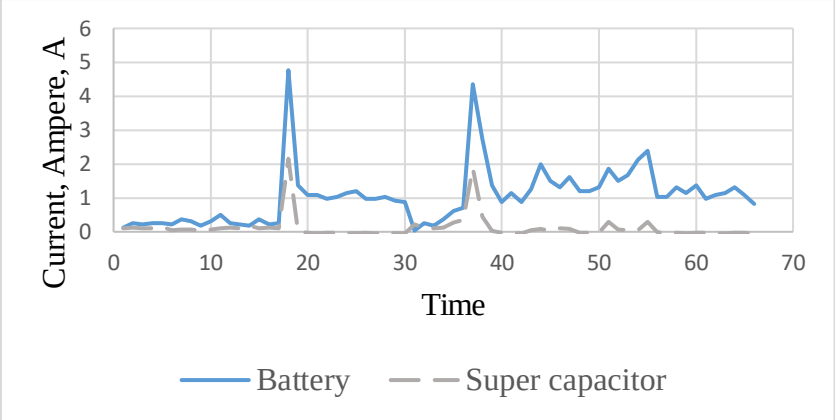

Figure 53: Dynamic approach system currents

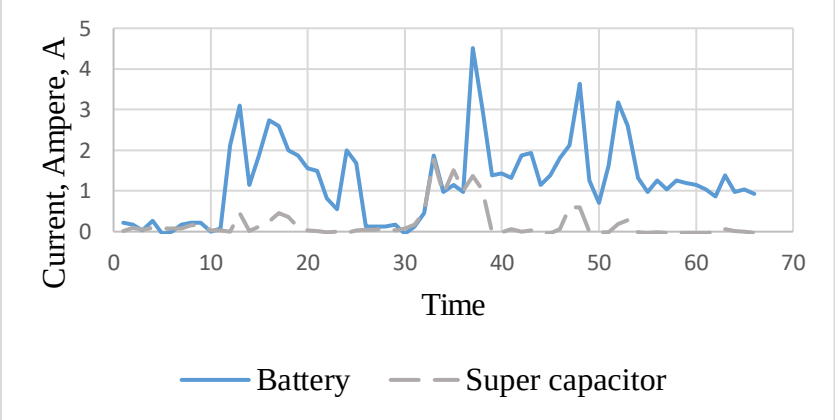

Figure 54: Heuristic approach system currents

System state of charges:

Figures 55, 56, and 57 display the system state-of-charges for the standard mode, dynamic approach, and heuristic approach respectively. The state-of-charge of the battery decreases most in the standard mode of operation, reaching 99.2% shown in Figure 57.

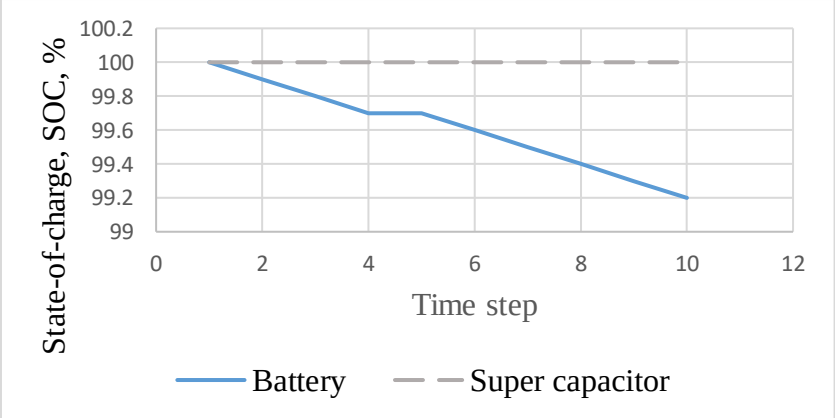

Figure 55: Standard mode state-of-charges

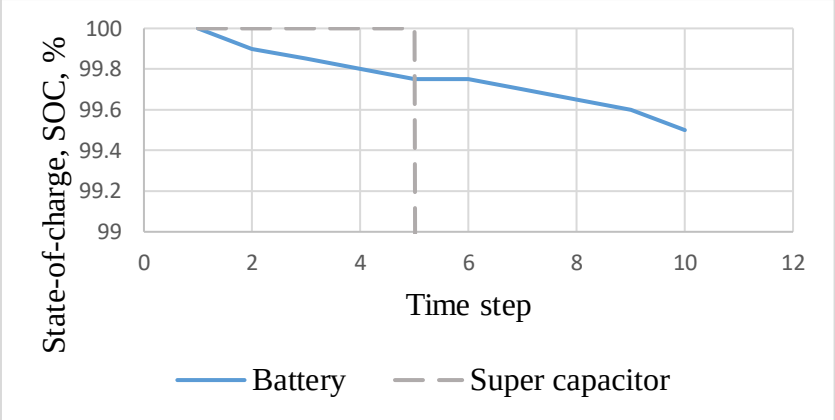

Figure 56: Dynamic programming state-of-charges

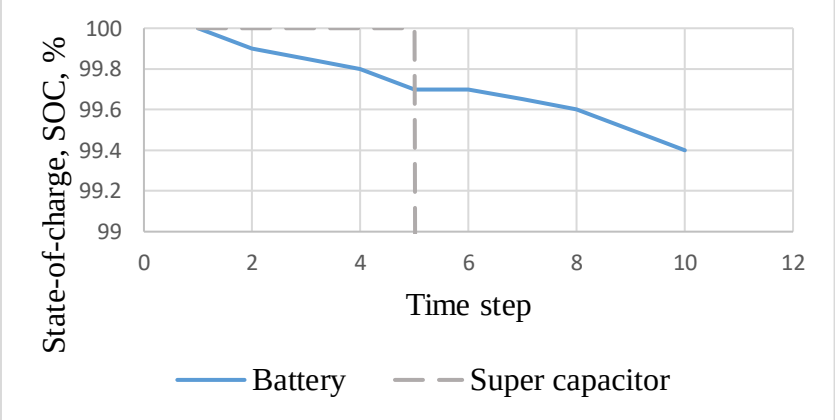

Figure 57: Heuristic approach state-of-charges

System power consumption:

In the experimental work, the standard mode of operation of the ground robot relied solely on the battery to meet the demand. On the other hand, the switching sequence of the dynamic approach chose to use the battery and super capacitor to meet the demand while the switching sequence of the heuristic approach chose all three sources. The switching sequence of the standard mode of operation resulted in the highest average power consumption from the sources, 33.3W. However, the dynamic approach generated a switching sequence that resulted in 5.5% decrease in the average power consumption compared to the standard mode of operation due to the voltage dynamics of the sources. Similarly, the switching sequence of the heuristic approach was able to reduce the average power consumption by 2.5% which is shown in Figure 58. Furthermore, the run time of the ground robot should increase since the system is less dependent on only one source to satisfy the demand.

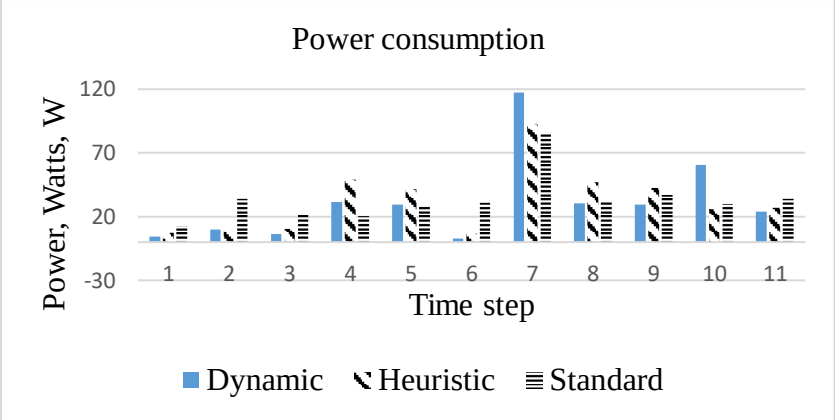

Figure 58: Power consumption comparison

Chapter 6: Conclusion

The system studied in this thesis is a drone containing four different power sources which are a hydrogen fuel cell, two batteries, a solar panel, and a super capacitor. The usage of each of the sources is controlled by turning connected switches on or off as needed to supply the demand of the drone. A mathematical model was developed for the efficient energy management of the integrated sources in the drone, generating an optimal switching sequence between the sources to increase the flight time and distance traveled. The mathematical model captures the essential details of the sources used in the drone are modeled while accounting for their unique characteristics and behaviors. Two methods have been developed to solve for the optimal switching sequence.

The first method uses a dynamic approach to minimize the running cost of the system by generating a switching sequence. This method was primarily tested on Lingo using the equations developed in the mathematical model. The dynamic algorithm was capable of generating a switching sequence which minimized the running cost of the drone, while the standard mode of operation was failing to provide the needed power. The algorithm was also able to prolong the flight time of the drone by charging the batteries and super capacitor as needed depending on the demand profile. The second method uses a heuristic approach, where a set of rules were used to generate the switching sequence. The heuristic algorithm was primarily tested on Matlab also using the equations developed in the mathematical model. The switching sequences generated by the heuristic algorithm were also able to prolong the flight time of the drone and minimize the running cost of the system but not as well as those of the dynamic approach. The switching sequences generated by the dynamic approach resulted in an average power consumption that was on average 9% lower than those of the heuristic approach. However, the main advantage introduced by the heuristic algorithm was the short computational time needed to generate the switching sequence between the sources. Also, the developed algorithms have been implemented offline before running the system, but have the capability to be implemented online. To be implemented online, the algorithms would require constant readings of the system's behavior and demand in order to generate the optimal switching sequence.

Additionally, the dynamic approach and the heuristic approach were tested on a ground robot built in AUS. Both approaches were able to generate switching sequences that minimize the running cost of the system and reduce the average power consumption across the sources, due to the voltage dynamics of the sources. However the switching sequence of the dynamic approach resulted in the greatest reduction in the average power consumption; 5.5% lower average power consumption compared to the standard mode of operation of the robot. The switching sequence of the heuristic approach was also able to reduce the average power consumption by 2.5% compared to the standard mode of operation.

Moreover, the developed algorithms were able to generate a switching sequence to manipulate the various sources integrated in the drone. Thus, resulting in increasing the flight time and travel distance of the drone as shown by the comparison of both the dynamic and heuristic approach to the standard mode of operation. Furthermore, limitations faced in this work include the length of the simulations conducted. Due to the large computing power required, the simulations were conducted for only fifty seconds. However, with access to more computing power better switching sequences could be generated that provide a further reduction in the running cost of the system. Additionally future work could include the real-time management of the sources integrated in the drone, alongside continuous readings of the behavior of the system while the drone is inflight. By implementing the real-time management of the sources, the system could become more responsive to fluctuations in the demand.

References:

[1] Globalfootprints.org. (1992). 'What is sustainability'. [online] Available at: http://www.globalfootprints.org/sustainability [Accessed 18 Oct. 2017].

[2] A. A. Malikopoulos, "Supervisory Power Management Control Algorithms for Hybrid Electric Vehicles: A Survey," *IEEE Transactions on Intelligent Transportation Systems*, vol. 15, no. 5, pp. 1869–1885, 2014.

[3] X. Hu, N. Murgovski, L. M. Johannesson, and B. Egardt, "Optimal Dimensioning and Power Management of a Fuel Cell/Battery Hybrid Bus via Convex Programming," *IEEE/ASME Transactions on Mechatronics*, vol. 20, no. 1, pp. 457–468, 2015.

[4] A. Naamane and N. Msirdi, "Improving Multiple Source Power Management Using State Flow Approach," *Sustainability in Energy and Buildings Smart Innovation, Systems and Technologies*, vol. 22, pp. 779–785, 2013.

[5] Boutilier, J.J., Brooks, S.C., Byers, A., Buick, J.E., Cheskes, S., Chan, T.C., Janmohamed, A., Morrison, L.J., Schoellig, A.P., & Zhan, C, "Optimizing a Drone Network to Deliver Automated External Defibrillators," *Circulation*, vol.135, no. 25, pp. 2454-2465, 2017.

[6] Christopher Masjosthusmann, Ulrich Köhler, Nikolaus Decius, Ulrich Büker, "A vehicle energy management system for a Battery Electric Vehicle", *2012 IEEE Vehicle Power and Propulsion Conference (VPPC)*, pp. 339-344, 2012.

[7] J. Lee, "Optimization of a modular drone delivery system," *2017 Annual IEEE International Systems Conference (SysCon)*, 2017.

[8] S. M. Ferrandez, T. Harbison, T. Weber, R. Sturges, and R. Rich, "Optimization of a truck-drone in tandem delivery network using k-means and genetic algorithm," *Journal of Industrial Engineering and Management*, vol. 9, no. 2, pp. 374, 2016.

[9] J. P. Torreglosa, P. Garcia, L. M. Fernandez, and F. Jurado, "Predictive Control for the Energy Management of a Fuel-Cell–Battery–Supercapacitor Tramway," *IEEE Transactions on Industrial Informatics*, vol. 10, no. 1, pp. 276–285, 2014.

[10] S. Xie, J. Peng, and H. He, "Plug-In Hybrid Electric Bus Energy Management Based on Stochastic Model Predictive Control," *Energy Procedia*, vol. 105, pp. 2672–2677, 2017.

[11] X. Hu, N. Murgovski, L. M. Johannesson, and B. Egardt, "Optimal Dimensioning and Power Management of a Fuel Cell/Battery Hybrid Bus via Convex Programming," *IEEE/ASME Transactions on Mechatronics*, vol. 20, no. 1, pp. 457–468, 2015.

[12] S. Hadj-Said, G. Colin, A. Ketfi-Cherif, and Y. Chamaillard, "Convex Optimization for Energy Management of Parallel Hybrid Electric Vehicles," *IFAC-PapersOnLine*, vol. 49, no. 11, pp. 271–276, 2016.

[13] J. P. F. Trovao, V. D. N. Santos, C. H. Antunes, P. G. Pereirinha, and H. M. Jorge, “A Real-Time Energy Management Architecture for Multisource Electric Vehicles,” *IEEE Transactions on Industrial Electronics*, vol. 62, no. 5, pp. 3223–3233, 2015.

[14] J. P. F. Trovao, M.-A. Roux, E. Menard, and M. R. Dubois, “Energy- and Power-Split Management of Dual Energy Storage System for a Three-Wheel Electric Vehicle,” *IEEE Transactions on Vehicular Technology*, vol. 66, no. 7, pp. 5540–5550, 2017.

[15] D. Zhou et al., “Online energy management strategy of fuel cell hybrid electric vehicles based on time series prediction,” *2017 IEEE Transportation Electrification Conference and Expo (ITEC)*, 2017.

[16] Z. Chen, W. Liu, Y. Yang, and W. Chen, “Online Energy Management of Plug-In Hybrid Electric Vehicles for Prolongation of All-Electric Range Based on Dynamic Programming,” *Mathematical Problems in Engineering*, vol. 2015, pp. 1–11, 2015.

[17] S. Park, L. Zhang and S. Chakraborty, "Battery assignment and scheduling for drone delivery businesses," *2017 IEEE/ACM International Symposium on Low Power Electronics and Design (ISLPED)*, pp. 1-6, 2017.

[18] S. Umetani, Y. Fukushima, and H. Morita, “A linear programming based heuristic algorithm for charge and discharge scheduling of electric vehicles in a building energy management system,” *Omega*, vol. 67, pp. 115–122, 2017.

[19] M. Chen and G. Rincon-Mora, “Accurate Electrical Battery Model Capable of Predicting Runtime and I–V Performance,” *IEEE Transactions on Energy Conversion*, vol. 21, no. 2, pp. 504–511, 2006.

[20] E. Schaltz, A. Khaligh, and P. Rasmussen, “Influence of Battery/Ultracapacitor Energy-Storage Sizing on Battery Lifetime in a Fuel Cell Hybrid Electric Vehicle,” *IEEE Transactions on Vehicular Technology*, vol. 58, no. 8, pp. 3882–3891, 2009.

[21] J. Bernard, S. Delprat, F. Buchi, and T. Guerra, “Fuel-Cell Hybrid Powertrain: Toward Minimization of Hydrogen Consumption,” *IEEE Transactions on Vehicular Technology*, vol. 58, no. 7, pp. 3168–3176, 2009.

[22] J. Pukrushpan, Modeling and control of fuel cell systems and fuel processors. PhD [Dissertation]. Michigan, USA: University of Michigan, 2003.

[23] R. Spyker and R. Nelms, “Classical equivalent circuit parameters for a double-layer capacitor,” *IEEE Transactions on Aerospace and Electronic Systems*, vol. 36, no. 3, pp. 829–836, 2000.

[24] Z. Amjadi and S. Williamson, “Power-Electronics-Based Solutions for Plug-in Hybrid Electric Vehicle Energy Storage and Management Systems,” *IEEE Transactions on Industrial Electronics*, vol. 57, no. 2, pp. 608–616, 2010.

[25] M. B. Camara, B. Dakyo, and H. Gualous, “Polynomial Control Method of DC/DC Converters for DC-Bus Voltage and Currents Management—Battery and Supercapacitors,” *IEEE Transactions on Power Electronics*, vol. 27, no. 3, pp. 1455–1467, 2012.

[26] “Fuel cell materials - Sandvik Materials Technology,” - Sandvik Materials Technology. [Online]. Available: https://www.materials.sandvik/en/applications/fuel-cells/fuel-cell-materials/. [Accessed: 13-Apr-2018].

[27] Saaty, T.L., 1980. *The Analytic Hierarchy Process. McGraw-Hill*, New York.

[28] S. Eaves and J. Eaves, “A cost comparison of fuel-cell and battery electric vehicles,” *Journal of Power Sources*, vol. 130, no. 1-2, pp. 208–212, 2004.

[29] J. Kunze, O. Paschos, and U. Stimming, “Fuel Cell Comparison to Alternate Technologies,” *Fuel Cells*, vol. 1, pp. 77–95, Jan. 2012.

[30] “Cost Projection of State of the Art Lithium-Ion Batteries for Electric Vehicles Up to 2030,” *Energies*, vol. 10, no. 9, p. 1314, Jan. 2017.

[31] A. Banerjee and A. Roychoudhury, “Future of Mobile Software for Smartphones and Drones: Energy and Performance,” *2017 IEEE/ACM 4th International Conference on Mobile Software Engineering and Systems (MOBILESoft)*, 2017.

Appendix A

```
SETS:
Power / 1..10/ : PV, Pdemand, PB1, PB2, PFC, PC, PPV, SB1, SB2, SPV,
SC, SFC, CHB1, CHB2, CHC, SOCB1, SOCB2, SOCC,VC;
ENDSETS
!Objective Function;
Min = @Sum (Power(i):(WB1*(PB1(i)*(1-CHB1(i))))+(WB2*(PB2(i)*(1-
CHB2(i))))+(WC*(PC(i)*(1-CHC(i))))+WFC*PFC(i)+WPV*PPV(i));
@for( Power(j):
!Initializing the decision variables to binary variables;
            @bin(SB1(j));
            @bin(SB2(j));
            @bin(CHB1(j));
            @bin(CHB2(j));
            @bin(SC(j));
            @bin(CHC(j));
            @bin(SPV(j));
            @bin(SFC(j));
SB1(j)*CHB1(j)=0;
!This constraint ensures that the first battery can only either be
charging or discharging or left idle;
SB2(j)*CHB2(j)=0;
!This constraint ensures that the second battery can only either be
charging or discharging or left idle;
SC(j)*CHC(j)=0;
!This constraint ensures that the super capacitor can only either be
charging or discharging or left idle;
CHB1(j)<= SPV(j);
!This constraint ensures that the first battery can only be charged
from the photovoltaic cell;
CHB2(j)<= SPV(j);
!This constraint ensures that the second battery can only be charged
from the photovoltaic cell;
CHB1(j)*CHB2(j)=0;
!This constraint ensures that only one batttery can be charged at a
time;
CHC(j)<= SPV(j);
!This constraint ensures that the super capacitor can only be charged
from the photovoltaic cell;
CHC(j)*CHB1(j)=0;
!This constraint ensures that the super capacitor cannot be charged
if the first battery is being charged;
CHC(j)*CHB2(j)=0;
!This constraint ensures that the super capacitor cannot be charged
if the second battery is being charged;
Pdemand(j)<= (PB1(j)*(1-CHB1(j)))+(PB2(j)*(1-CHB2(j)))+(PC(j)*(1-
CHC(j)))+PFC(j)+PPV(j);
!This constraint ensures that the power supplied is greater than or
equal to the power demanded by the system;
SOCB1(j) <= 100;
SOCB1(j) >= 30;
SOCB2(j) <= 100;
SOCB2(j) >= 30;
!These constraints ensure that the State of Charge of the batteries
is kept between 30% to 100%;);
!First iteration Calculations;
!Super capacitor;
VC(1)=((24*(1-@EXP(-6/tao)))*CHC(1))+(24*@EXP(-6/tao))*SC(1)+ 24*(1-
(SC(1)+CHC(1)));
PC(1) = 24*IC*(SC(1)+CHC(1));
!Batteries' State of Charge;
```

```
SOCB1(1) = ((-1/Cc)*IB1)*(SB1(1)-CHB1(1)*0.4)+100;
SOCB2(1) = ((-1/Cc)*IB1)*(SB1(1)-CHB1(1)*0.4)+100;
!Initial Super capacitor State of Charge;
SOCC(1)= 100;
!Power Supplied by the sources;
PB1(1) = VB1*IB1*(SB1(1)+CHB1(1));
PB2(1) = VB2*IB2*(SB2(1)+CHB2(1));
PPV(1)= SPV(1)*PV(1)*(1-(CHB1(1)+CHB2(1)+CHC(1)));!(1-(CHB1(1)))*(1-
CHB2(1))*(1-CHC(1));
PFC(1)= SFC(1)*VFC*IFC;
@for( Power(i) | i#NE#1:
!BATTERIES MODEL;
PB1(i) = VB1*IB1*(SB1(i)+CHB1(i));
PB2(i) = VB2*IB2*(SB2(i)+CHB2(i));
!PHOTOVOLTAIC CELL;
PPV(i)= SPV(i)*PV(i)*(1-(CHB1(i)+CHB2(i)+CHC(i)));!(1-CHB1(i))*(1-
CHB2(i))*(1-CHC(i));
!Fuel Cell;
PFC(i)= SFC(i)*VFC*IFC;
!Super Capacitor;
VC(i)=(24*(1-@EXP(-6/tao)))*CHC(i)+ (VC(i-1)*@EXP(-6/tao))*SC(i)+
(VC(i-1)*(1-(SC(i)+CHC(i))));
PC(i) = VC(i-1)*IC*(SC(i)+CHC(i));
!State of Charge for the Batteries & Super Capacitor;
SOCB1(i) = ((-1/Cc)*IB1)*(SB1(i)-CHB1(i)*0.4)+SOCB1(i-1);
SOCB2(i) = ((-1/Cc)*IB2)*(SB2(i)-CHB2(i)*0.4)+SOCB2(i-1);
SOCC(i)= (VC(i)/VCrated)*100;       );
DATA:
WB1=0.22;
WB2=0.22;
WC=0.20;
WFC=0.11;
WPV=0.13;
VB1= 22.4;
VB2= 22.4;
IB1= 165;
IB2= 165;
Cc= 10;
R=0.12;
C=3;
VCrated= 24;
IC= 200;
tao= 0.36;
VFC= 21;
IFC= 10;
PV= 120,120,120,120,120,120,120,120,120,120;
Pdemand=200,2000,3500,3800,3800,3000,4000,4000,2000,200;

ENDDATA
```

Appendix B

```
!Data;
PV= [120,120,120,120,120,120,120,120,120,120];
Pdemand=[1000,1000,1000,3500,3500,3500,2500,2500,2500,2500];
WB1=0.195;
WB2=0.195;
WC=0.27;
WFC=0.21;
WPV=0.13;
VB1= 22.4;
VB2= 22.4;
IB1= 165;
IB2= 165;
Cc= 10;
R=0.12;
C=3;
VCrated= 24;
IC= 200;
tao= 0.36;
VFC= 21;
IFC= 10;
!intialization of matrices;
SC=zeros(1,10);
Sfc=zeros(1,10);
SB1=zeros(1,10);
SB2=zeros(1,10);
Spv=zeros(1,10);
CHB1=zeros(1,10);
CHB2=zeros(1,10);
CHC=zeros(1,10);
PB1=zeros(1,10);
PB2=zeros(1,10);
Pfc=zeros(1,10);
Ppv=zeros(1,10);
PC=zeros(1,10);
SOCB1=[100,0 , 0, 0, 0, 0, 0, 0,0 ];
SOCB2=[100,0 , 0, 0, 0, 0, 0, 0,0 ];
SOCC=[100,0 , 0, 0, 0, 0, 0, 0,0 ];
VC=[24,0 , 0, 0, 0, 0, 0, 0,0 ];
obj=zeros(1,10);
!Calculating the power supplied by each of the sources;
P_FC= VFC*IFC;
P_B1 = VB1*IB1;
P_B2 = VB2*IB2;
P_PV= PV;
!First Iteration;
if (Pdemand(1)>200)

                if Pdemand(1) < P_FC
                    Sfc(1)=1;


                elseif (Pdemand(1) < P_FC + P_PV)
                         Sfc(1)=1;
                          Spv(1)=1;

                 elseif (SOCB1(1) > 47)

                       if (Pdemand(1) < P_FC +P_PV +P_B1)
```

```
                                Sfc(1)=1;
                                 Spv(1)=1;
                                 SB1(1)=1;

                           elseif (SOCB2(1) > 47)
                                   Sfc(1)=1;
                                    Spv(1)=1;
                                    SB1(1)=1;
                                    SB2(1)=1;
                           elseif (SOCC(1) == 100)
                                    Sfc(1)=1;
                                    Spv(1)=1;
                                    SB1(1)=1;
                                    SC(1)=1;
                           end
                      elseif (SOCB2(1) > 47)
                                    Sfc(1)=1;
                                    Spv(1)=1;
                                    SB2(1)=1;
                      elseif (SOCC(1)==100)
                                    Sfc(1)=1;
                                    Spv(1)=1;
                                    SC(1)=1;

                    end
end
           if (Pdemand(1)<= 200)
                                Sfc(1)=1;

                            if (SOCC(1) < 99)
                                        Spv(1)=1;
                                        CHC(1)=1;

                            elseif (SOCB1(1) < 100)
                                       Spv(1)=1;
                                       CHB1(1)=1;

                           elseif (SOCB2(1) < 100)
                                       Spv(1)=1;
                                       CHB2(1)=1;
                            end

                                VC(1)=(24*(1-exp(-6/tao)))*CHC(1)+ (24
*exp(-6/tao))*SC(1)+ (24 *(1-(SC(1)+CHC(1))));
                                PC(1) = 24*IC*(SC(1)+CHC(1));
          end
!Power supplied by the batteries;
PB1(1) = VB1*IB1*(SB1(1)+CHB1(1));
PB2(1) = VB2*IB2*(SB2(1)+CHB2(1));
!Power supplied by the PV;
PPV(1)= Spv(1)*PV(1)*(1-(CHB1(1)+CHB2(1)+CHC(1)));
!Power supplied by the Fuel Cell;
PFC(1)= Sfc(1)*VFC*IFC;
!State of charge of the batteries & super capacitor;
SOCB1(1) = ((-1/Cc)*IB1)*(SB1(1)-CHB1(1)*0.4)+100;
SOCB2(1) = ((-1/Cc)*IB2)*(SB2(1)-CHB2(1)*0.4)+100;
SOCC(1)= (VC(1)/VCrated)*100;
!Objective function value for the first iteration;
obj(1) = (WB1*(PB1(1)*(1-CHB1(1))))+(WB2*(PB2(1)*(1-
CHB2(1))))+(WC*(PC(1)*(1-CHC(1))))+WFC*PFC(1)+WPV*PPV(1);
```

```
!Remaining iterations;
for i=2:10

        if (Pdemand(i)>200)
                if (Pdemand(i)>1.3*Pdemand(i-1))
                    if(SOCC(i-1) > 50)
                          SC(i)=1;
                    end
                end
               VC(i)=(24*(1-exp(-6/tao)))*CHC(i)+ (VC(i-1)*exp(-
6/tao))*SC(i)+ (VC(i-1)*(1-(SC(i)+CHC(i))));
               PC(i) = VC(i-1)*IC*(SC(i)+CHC(i));

                if Pdemand(i)-PC(i) < P_FC
                    Sfc(i)=1;

                elseif (Pdemand(i)-PC(i) < P_FC + P_PV)
                         Sfc(i)=1;
                          Spv(i)=1;


                elseif  (SOCB1(i-1) > 47)
                        if (Pdemand(i)-PC(i) < P_FC +P_PV +P_B1)
                             Sfc(i)=1;
                              Spv(i)=1;
                              SB1(i)=1;

                        elseif (SOCB2(i-1) > 47)
                                Sfc(i)=1;
                                 Spv(i)=1;
                                 SB1(i)=1;
                                 SB2(i)=1;

                        elseif (SOCC(i-1) == 100)
                                 Sfc(i)=1;
                                 Spv(i)=1;
                                 SB1(i)=1;
                                 SC(i)=1;
                        end

                elseif  (SOCB2(i-1) > 47)
                   if (Pdemand(i)-PC(i) < P_FC +P_PV +P_B2)
                             Sfc(i)=1;
                              Spv(i)=1;
                              SB2(i)=1;
                   elseif (SOCC(i-1) == 100)
                                 Sfc(i)=1;
                                 Spv(i)=1;
                                 SB2(i)=1;
                                 SC(i)=1;
                   end
               end
        end


                    if (Pdemand(i)<= 200)
                            Sfc(i)=1;

                        if (SOCC(i-1) < 99)
```

```
                                        Spv(i)=1;
                                        CHC(i)=1;

                            elseif (SOCB1(i-1) < 100)
                                        Spv(i)=1;
                                        CHB1(i)=1;

                           elseif (SOCB2(i-1) < 100)
                                        Spv(i)=1;
                                        CHB2(i)=1;
                            end

                                    VC(i)=(24*(1-exp(-6/tao)))*CHC(i)+
(VC(i-1)*exp(-6/tao))*SC(i)+ (VC(i-1)*(1-(SC(i)+CHC(i))));
                                    PC(i) = VC(i-1)*IC*(SC(i)+CHC(i));
                       end

!Power supplied by the batteries;
PB1(i) = VB1*IB1*(SB1(i)+CHB1(i));
PB2(i) = VB2*IB2*(SB2(i)+CHB2(i));
!Power supplied by the PV;
PPV(i)= Spv(i)*PV(i)*(1-(CHB1(i)+CHB2(i)+CHC(i)));
!Power supplied by the Fuel Cell;
PFC(i)= Sfc(i)*VFC*IFC;
!State of charge of the batteries & super capacitor;
SOCB1(i) = ((-1/Cc)*IB1)*(SB1(i)-CHB1(i)*0.4)+SOCB1(i-1);
SOCB2(i) = ((-1/Cc)*IB2)*(SB2(i)-CHB2(i)*0.4)+SOCB2(i-1);
SOCC(i)= (VC(i)/VCrated)*100;
!Objective function value;
obj(i) = (WB1*(PB1(i)*(1-CHB1(i))))+(WB2*(PB2(i)*(1-
CHB2(i))))+(WC*(PC(i)*(1-CHC(i))))+WFC*PFC(i)+WPV*PPV(i);

end
```

Appendix C

- **Sensitivity Analysis of illustrative example 1 in section 5.1.**

This simulation represents the situation where a drone must travel to a certain location to pick up an object and continue to the drone's final destinations. During its flight, the drone faces turbulence causing fluctuations in the demand profile. The demand profile of this simulation is shown in Figure 59.

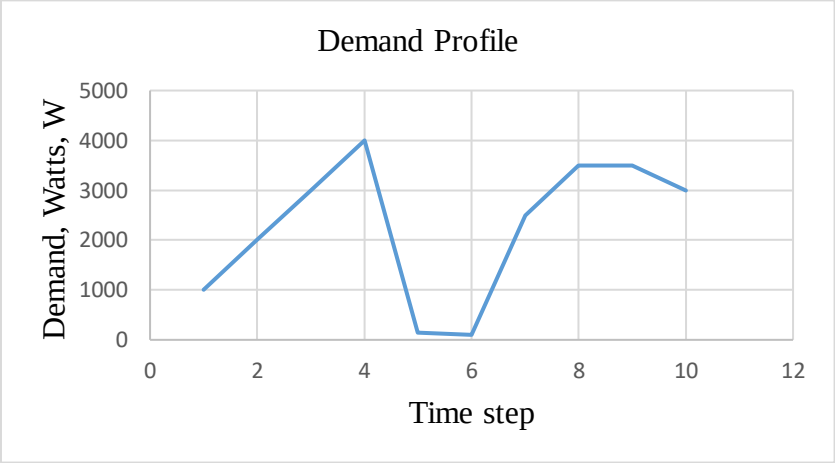

Figure 59: Demand profile for simulation 7

As shown in Figure 59, the drone starts traveling to the location were the object is located. At time period 4, the drone reaches the object's location and descends to pick up the object while dealing with turbulences. After the drone picks up the object it continues its flight to return to its base.

System voltages:

Figures 60 and 61 display the system voltages for both the dynamic approach and heuristic approach respectively. Similar to example 1, the switching sequence generated by the dynamic approach chose not to use the super capacitor while the heuristic approach did.

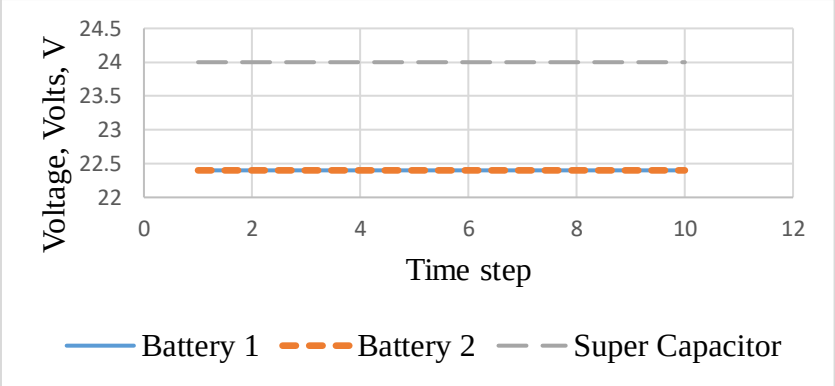

Figure 60: System voltages for dynamic approach

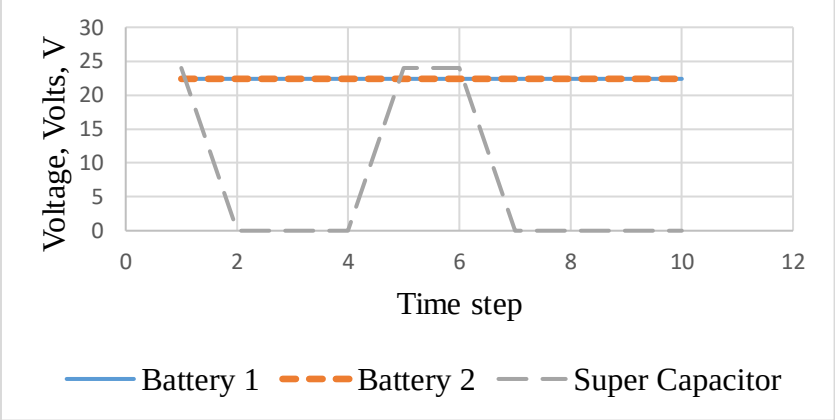

Figure 61: System voltages for heuristic approach

System currents:

Figures 62 and 63 display the system currents for both the dynamic and heuristic approach respectively. As the super capacitor was not used by the dynamic programming, the current remains 0 while the currents of the batteries vary as they are being used. However, in the heuristic approach both batteries and the super capacitor were used therefore their currents vary accordingly.

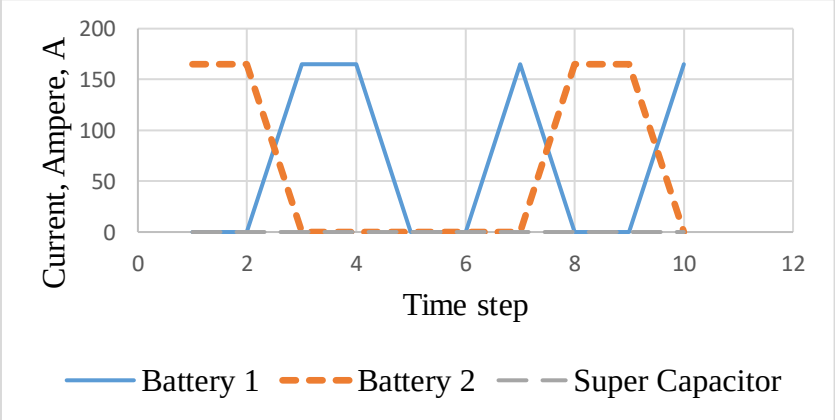

Figure 62: System currents for dynamic approach

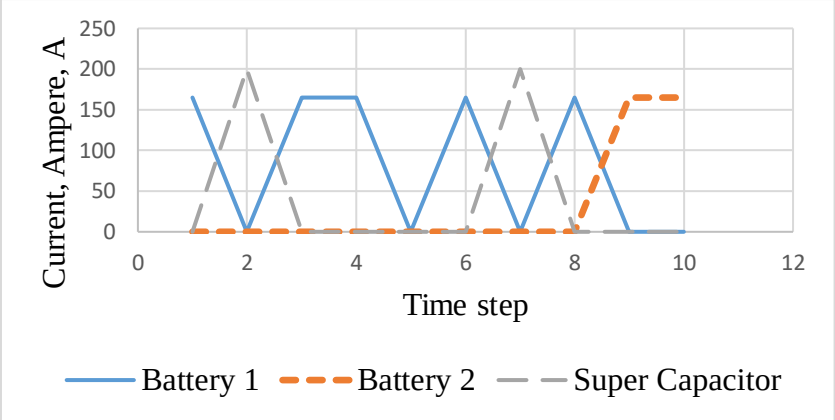

Figure 63: System currents for heuristic approach

System state-of-charges:

Figures 64 and 65 display the system state-of-charges for both the dynamic and heuristic approach respectively.

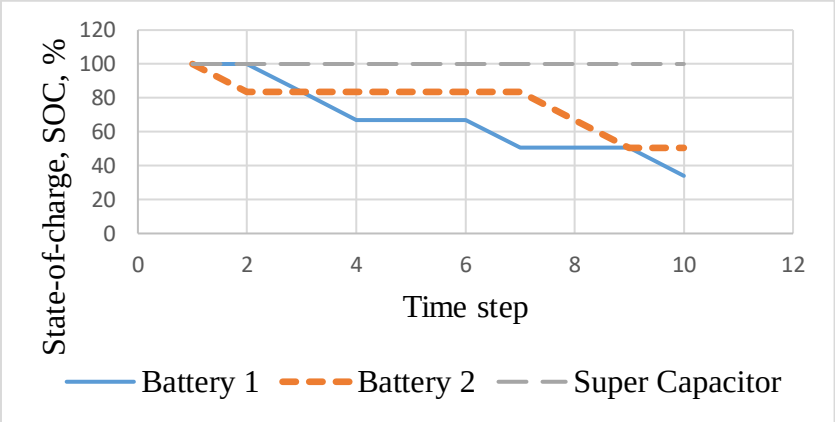

Figure 64: System state-of-charges for dynamic approach

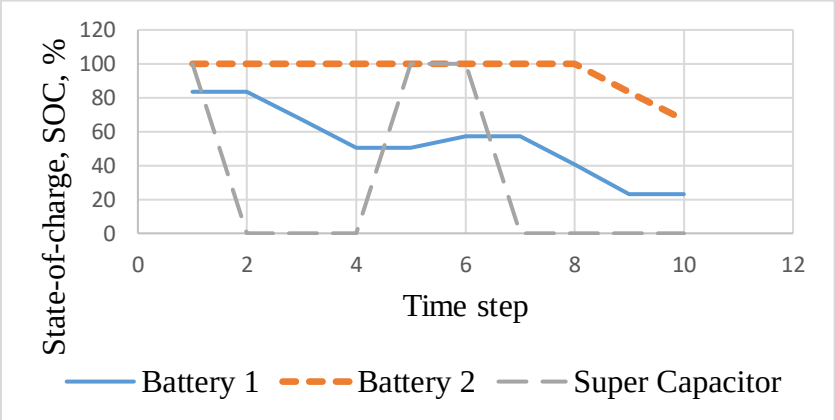

Figure 65: System state-of-charges for heuristic approach

System power consumption:

In the object pickup simulation with turbulence, both switching sequences of the dynamic and heuristic approach were able to meet the demand of the drone but the standard approach did not. The introduction of turbulence to the simulation caused an increased in the average power consumption and objective function value of solution provided by the dynamic approach; the objective function value increased from 6536.2 to 6582.360 and the average power consumption increased from 3720 W to 3800 W. However, the switching sequence of the heuristic approach did not cause an increase in the objective function since it was already supplying more than what the drone demanded which is shown in Figure 66.

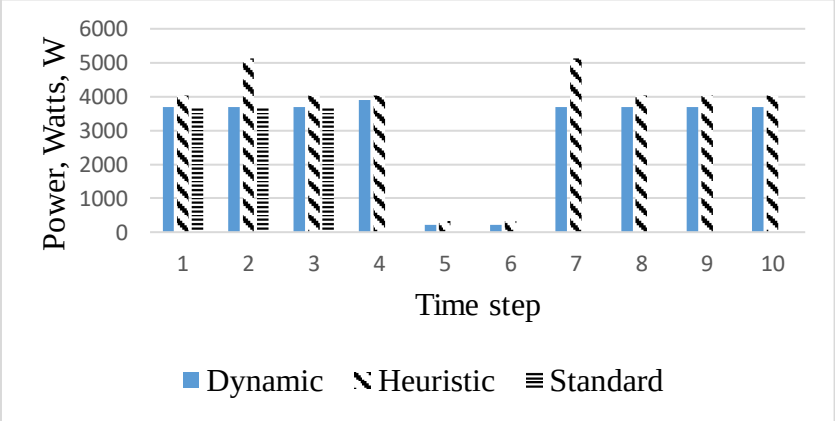

Figure 66: Power consumption comparison

- **Sensitivity Analysis of illustrative example 2 in section 5.2**

This simulation is similar to example 2 where the drone must maintain a certain height above the ground for a period of time. However, ideal conditions are considered where the drone does not face any distribution or turbulence while in flight. The demand profile of this simulation is shown in Figure 67.

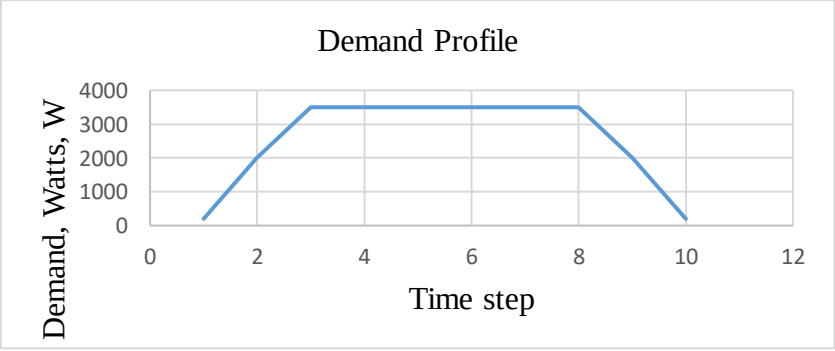

Figure 67: Demand Profile for Simulation 8

As shown in Figure 67, the drone starts ascending to the required height thus causing an increased in the demand of the drone. In time step 3, the drone reaches the required height and maintains it for 5 time steps. Finally, the drone begins to descend back to its base.

System voltages:

Figure 68 and 69 display the system voltages for both the dynamic and heuristic approach respectively. Similar to example 2, the switching sequence generated by the dynamic approach chose not to use the super capacitor while the heuristic approach did.

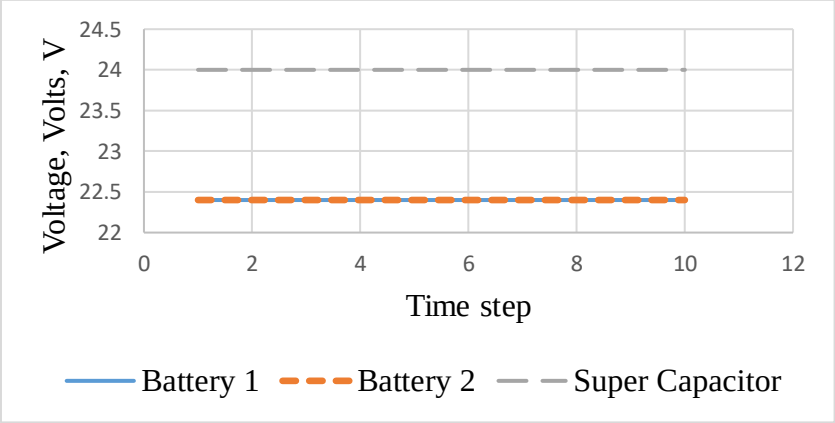

Figure 68: System voltages for dynamic approach

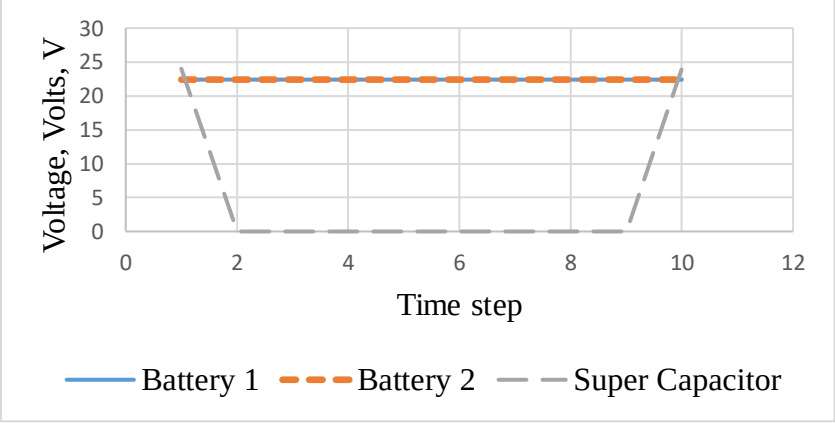

Figure 69: System voltages for heuristic approach

System currents:

Figures 70 and 71 display the system currents for both the dynamic and heuristic approach respectively. As the super capacitor was not used by the dynamic approach, the current remains 0 while the currents of the batteries vary as they are being used.

However, in the heuristic approach both batteries and the super capacitor were used therefore their currents vary accordingly.

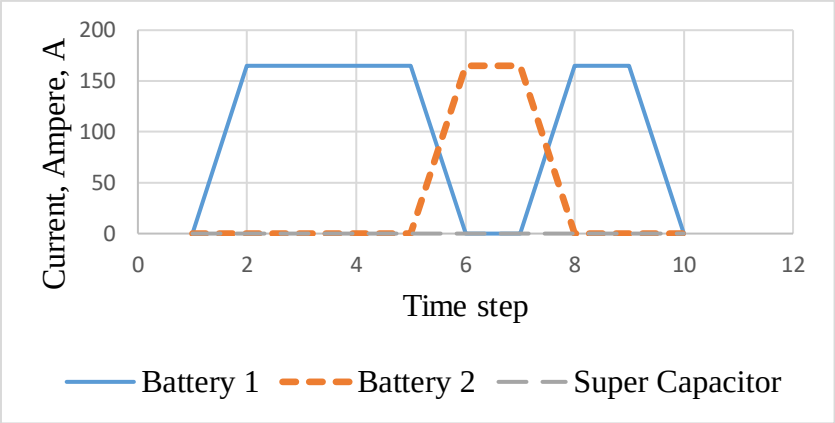

Figure 70: System currents for dynamic approach

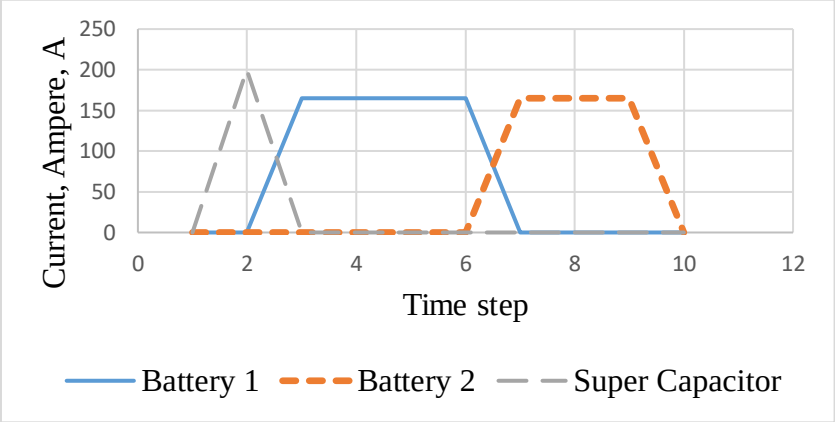

Figure 71: System currents for heuristic approach

System state-of-charges:

Figures 72 and 73 display the system state-of-charges for both the dynamic and heuristic approach respectively.

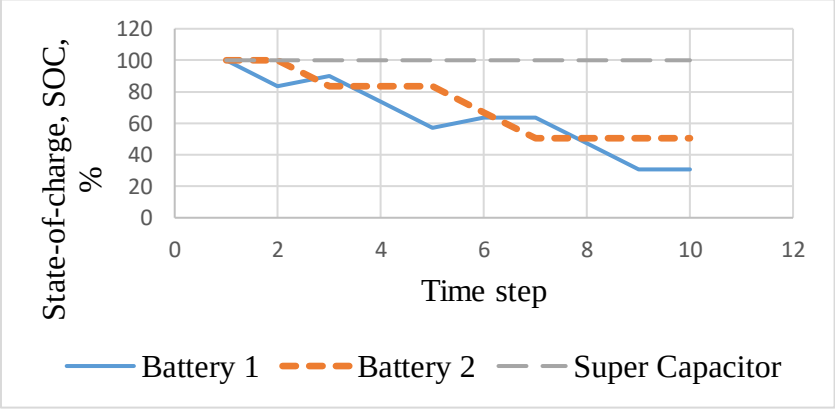

Figure 72: State-of-charges for dynamic approach

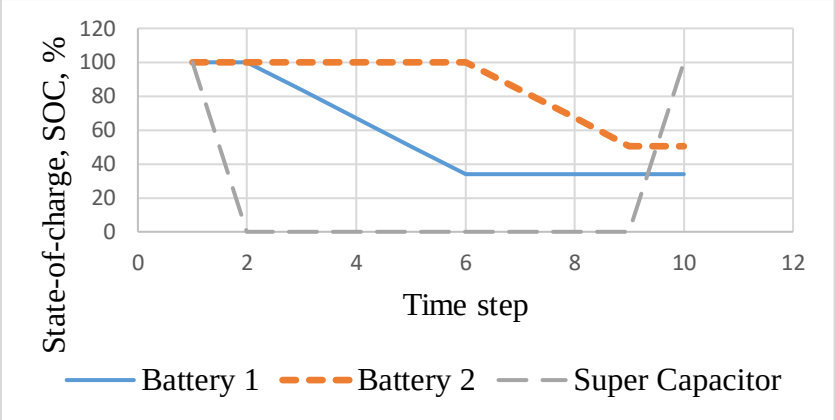

Figure 73: State-of-charges for heuristic approach

System power consumption:

In the altitude maintenance simulation with ideal conditions, both the switching sequences of the dynamic and heuristic approach were able to meet the demand of the drone but that of the standard approach did not. The removal of turbulence to the simulation caused a decrease in the average power consumption and objective function value in the switching sequences of the dynamic programming; the objective function value decreased from 6674.7 to 6651.2 and the average power consumption decreased from 3022.8 W to 2998.8 W. However, in the switching sequence of the heuristic approach did not cause a decrease in the objective function or average power consumption since the introduction turbulence wasn't significant enough to cause a change in the generated switching sequence which is shown in Figure 74.

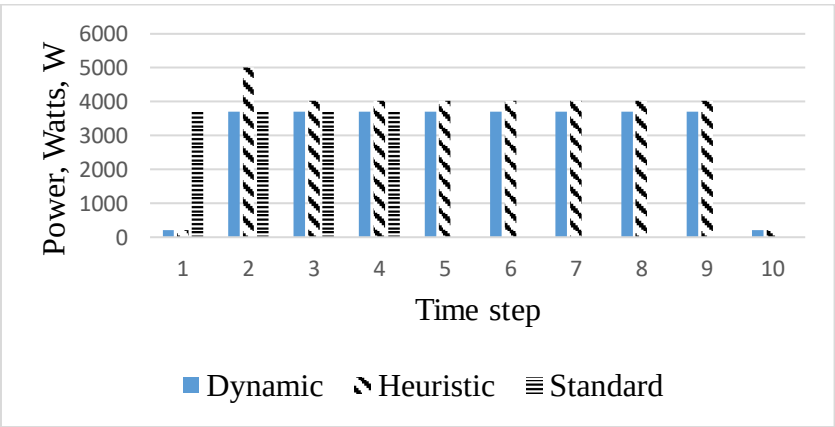

Figure 74: Power consumption comparison

- **Sensitivity Analysis of illustrative example 3 in section 5.3**

In this simulation, we changed the rating of the super capacitor to tailor it to the height of the spikes occurring in the demand as the drone descends and ascends to pick

up multiple objects just as in simulation 3. The size of the super capacitor has been changed from 3 Farads to 2 Farads, with a rating of 22 Volts. The demand profile of this simulation is shown in Figure 75.

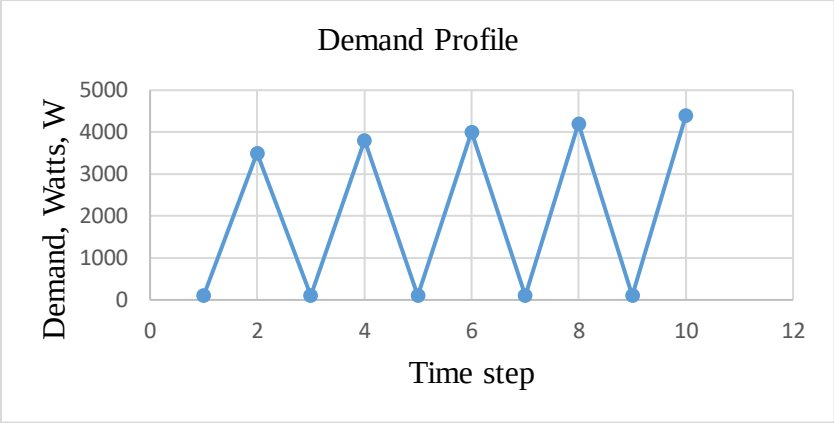

Figure 75: Demand profile for simulation 9

System voltages:

Figures 76 and 77 display the system voltages for both the dynamic and heuristic approach respectively. In this example, the switching sequence generated by the dynamic programming chose to mainly use the super capacitor as did the heuristic approach to meet the demand of the drone.

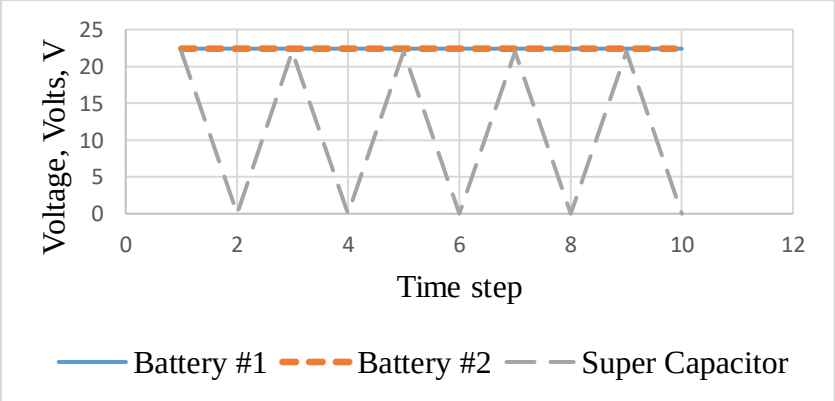

Figure 76: System voltages for dynamic approach

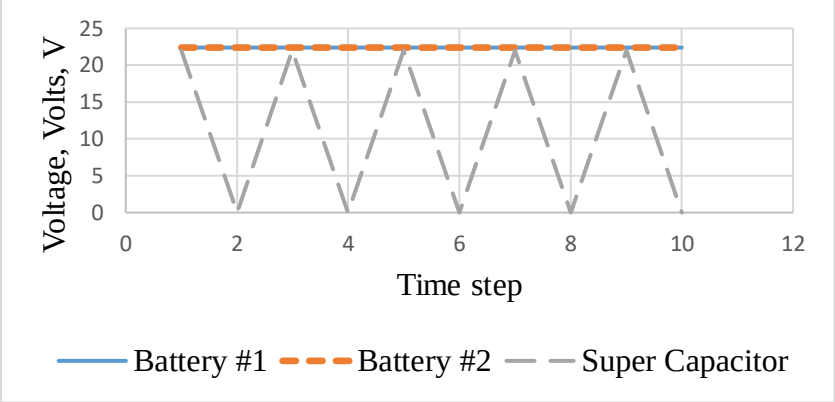

Figure 77: System voltages for heuristic approach

System currents:

Figures 78 and 79 display the system currents for both the dynamic and heuristic approach respectively. Also, the super capacitor's current varies in a similar manner to that of the drone's demand.

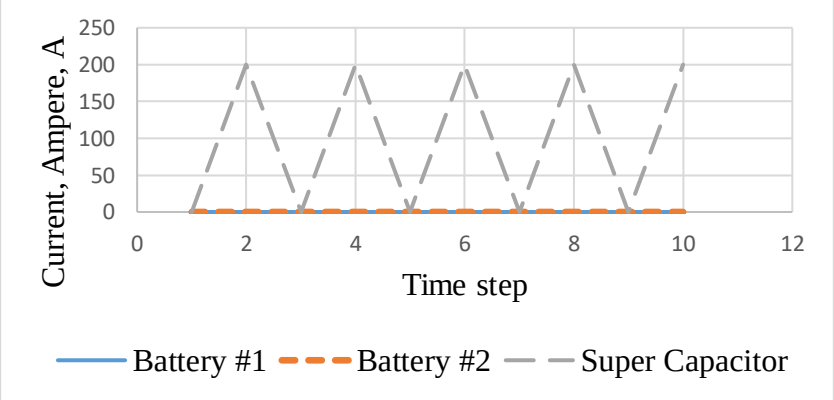

Figure 78: System currents for dynamic approach

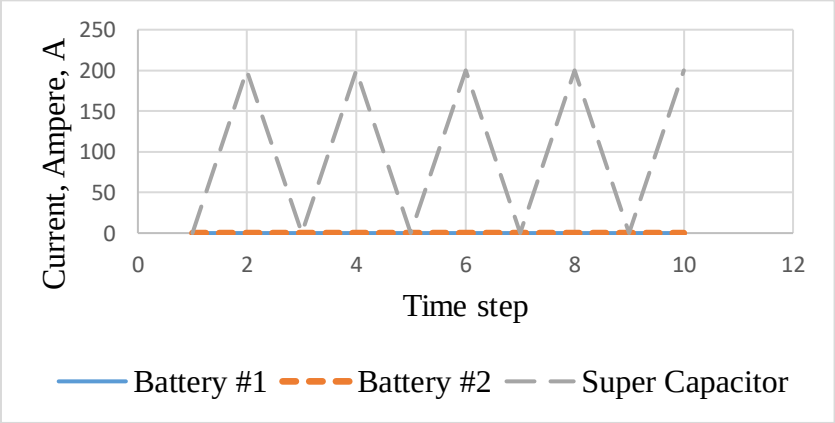

Figure 79: System currents for heuristic approach

System state of charges:

Figures 80 and 81 display the change in the state-of-charges of the batteries and super capacitor for both the dynamic and heuristic approach. Since the batteries were not using in this example, the state-of-charge of the batteries remains 100% while the super capacitor is charged and discharge multiple times to meet the demand.

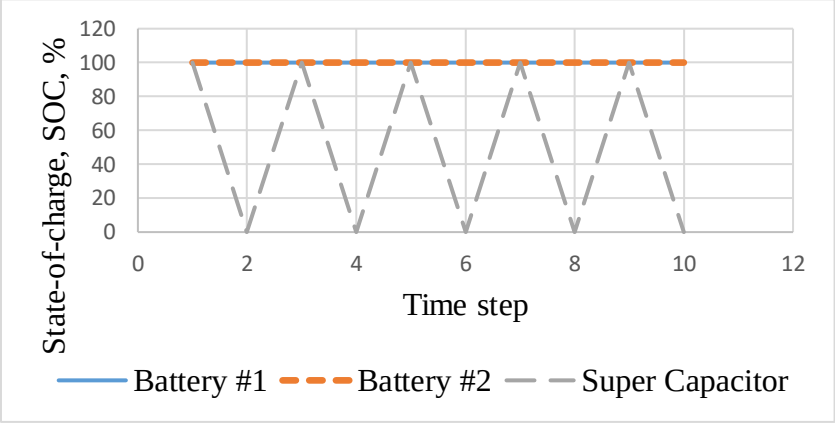

Figure 80: State-of-charges for dynamic approach

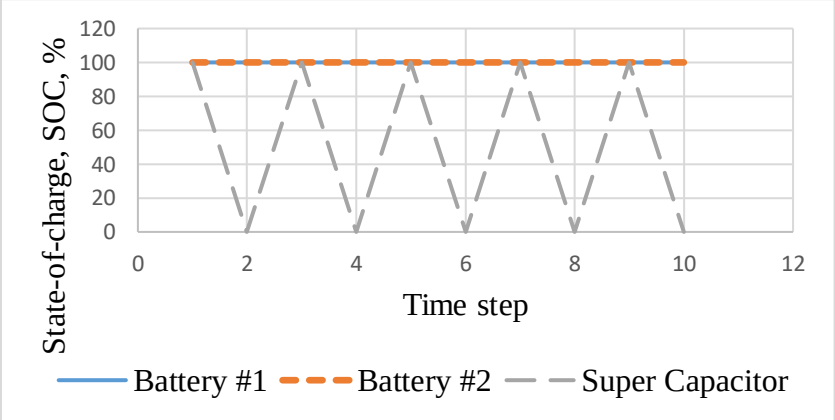

Figure 81: State-of-charges for heuristic approach

System power consumption:

The behavior of the system remains the same as in simulation 3 where the system relies on the super capacitor to meet the demand of the drone. However, less power was used from the system due to reducing the size of the super capacitor just enough to still be able to meet the spike demands. The objective function value dropped from 3499.2 to 3219.2 for the switching sequence of the dynamic approach, and from 3517.5 to 3237.5 for the switching sequence of the heuristic approach. Similarly the average power consumption for the solution provided by the dynamic approach dropped

from 2496W to 2296W and 2505 W to 2305 W for the solution provided by the heuristic approach which is shown in figure 82.

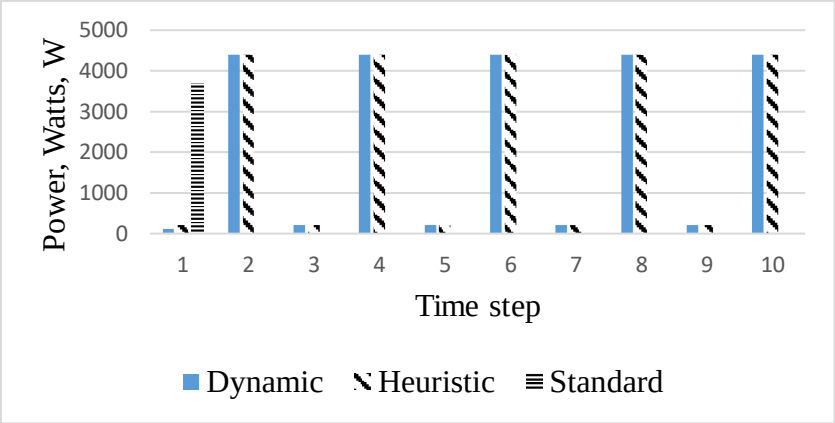

Figure 82: Power consumption comparison

Appendix D

Illustrative Example 1: Object Pickup

Figures 83 and 84 show the switching sequence generated by the dynamic and heuristic approach respectively.

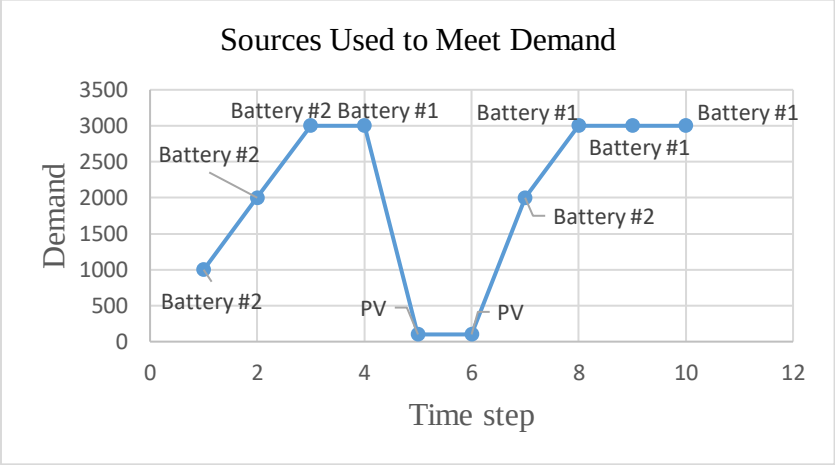

Figure 83: Dynamic approach switching sequence for simulation 1

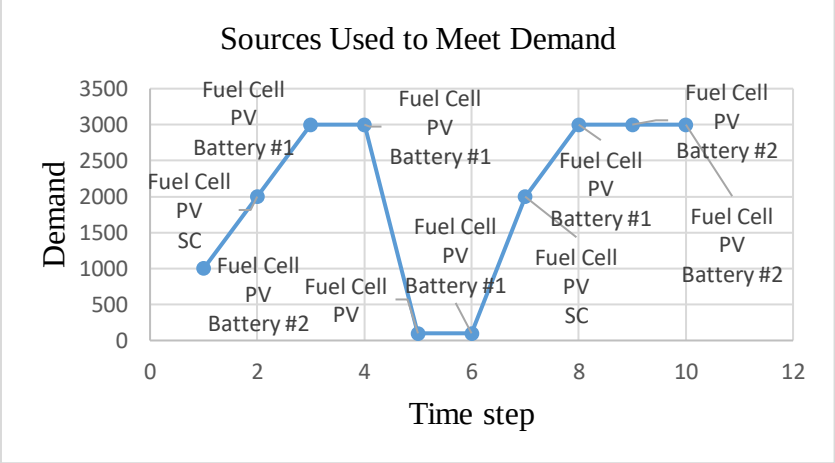

Figure 84: Heuristic approach switching sequence for simulation 1

Illustrative Example 2: Altitude Maintenance

Figures 85 and 86 show the switching sequence generated by the dynamic and heuristic approach respectively.

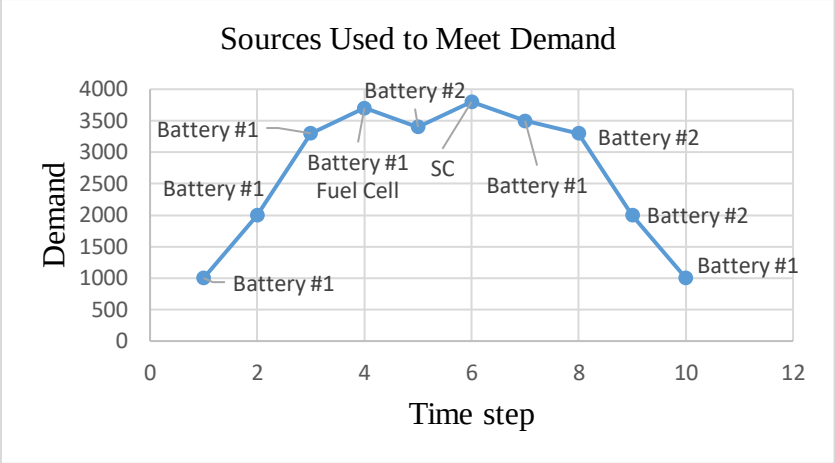

Figure 85: Dynamic approach switching sequence for simulation 2

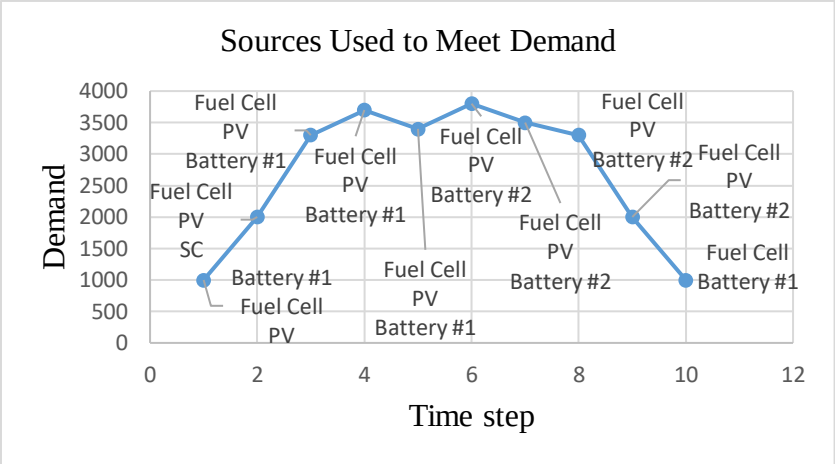

Figure 86: Heuristic approach switching sequence for simulation 2

Illustrative Example 3: Multiple object pickup

Figures 87 and 88 show the switching sequence generated by the dynamic and heuristic approach respectively.

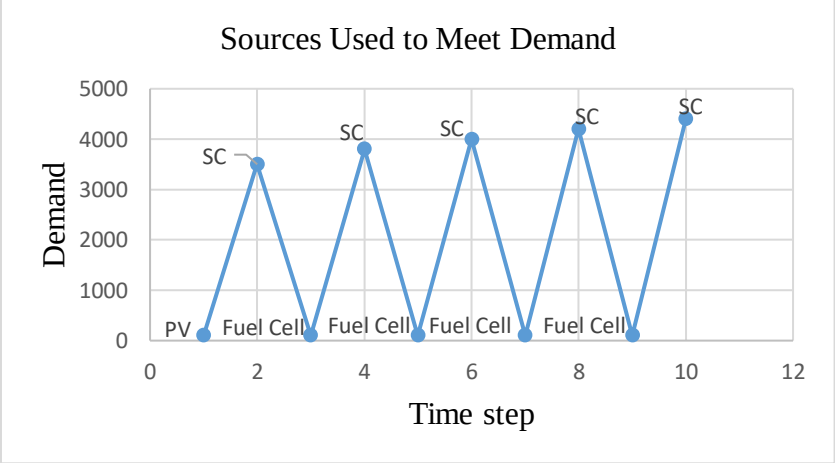

Figure 87: Dynamic approach switching sequence for simulation 3

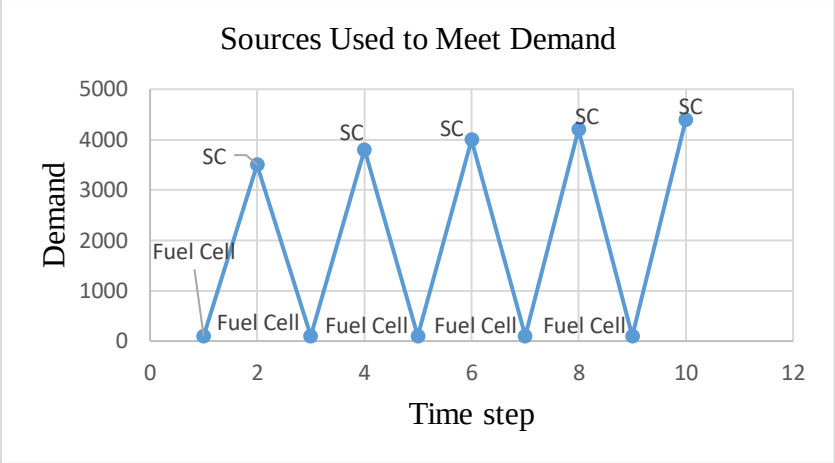

Figure 88: Heuristic approach switching sequence for simulation 3

Appendix E

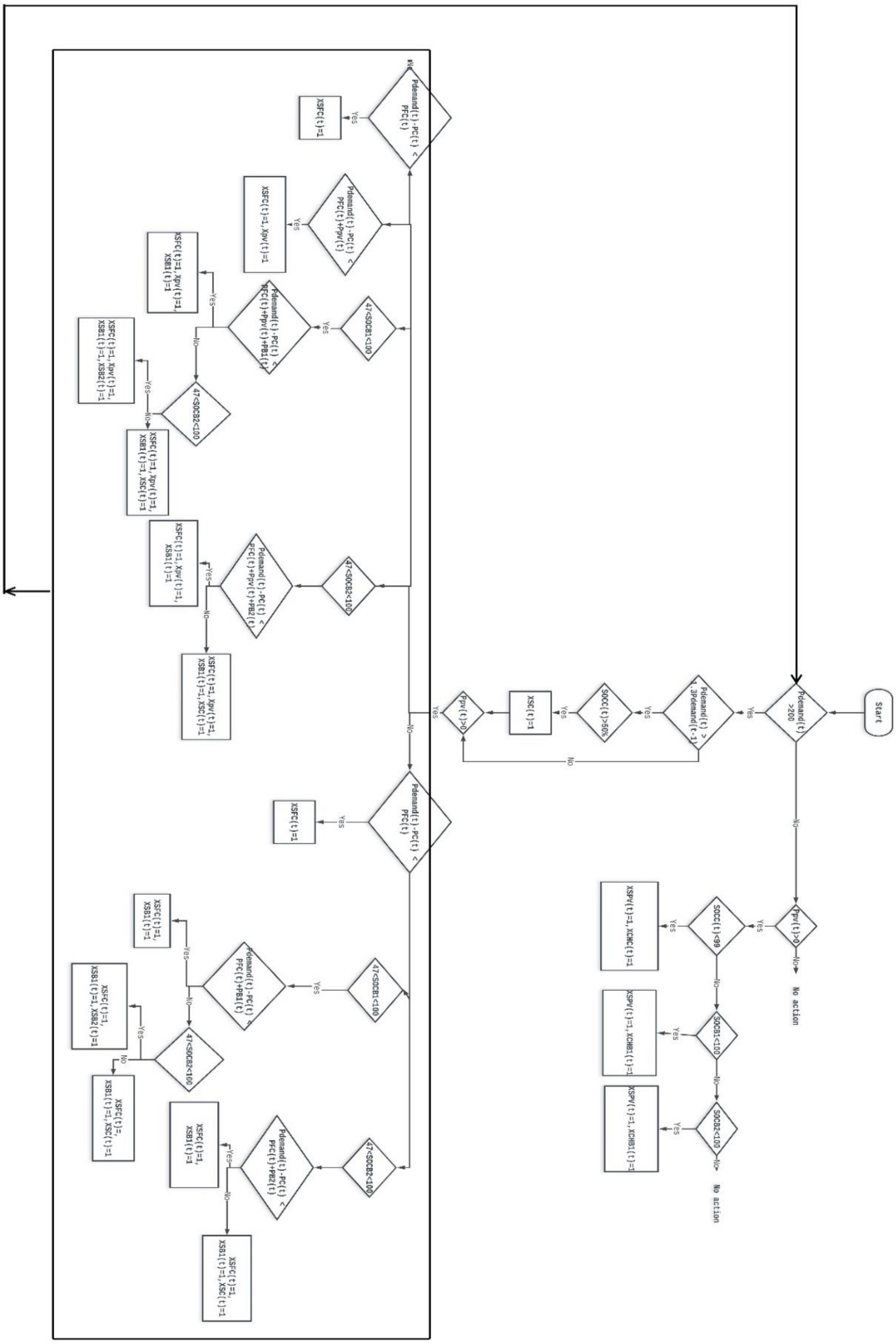

Figure 89: Heuristic approach flow chart

Vita

Omar Wasseem Salah was born in 1994, in Doha, Qatar. He was educated in local private schools and graduated from Global Academy International. He received a Merit Scholarship to the American University of Sharjah in Sharjah, United Arab Emirates, from which he graduated cum laude, in 2016. His degree was a Bachelor of Science in Electrical Engineering.

In September 2016, he joined the Engineering Systems Management master's program in the American University of Sharjah as a graduate teaching assistant. His research interests are in energy management.